Available online at www.sciencedirect.com
SCIENCE DIRECT®
Coordination Chemistry Reviews 249 (2005) 1957–1985
COORDINATION CHEMISTRY REVIEWS
www.elsevier.com/locate/ccr

Review

Carbon–fluorine bond activation by platinum group metal complexes

Hugo Torrens *

National University of Mexico, F. de Química, UNAM. Cd. Universitaria, 04510 México D.F., Mexico

Received 8 September 2004; received in revised form 8 December 2004; accepted 27 January 2005
Available online 12 March 2005

Contents

1. Introduction and scope 1957
2. Ruthenium 1958
3. Osmium 1961
4. Rhodium 1962
5. Iridium 1970
6. Palladium 1977
7. Platinum 1980
8. Final remarks 1982
Acknowledgements 1984
References 1984

Abstract

This review is focused on carbon─fluorine bond activation taking place at platinum group metal – PGM = Ru, Os, Rh, Ir, Pd and Pt – coordination compounds. It will specifically address the relevant examples in the area of fluorocarbon coordination to PGM leading to, at least, one C─F bond cleavage by surveying the work reported since 1994, covering the literature up to August 2004.

Keywords: Carbon─fluorine bond; Platinum group metal; Ruthenium; Osmium; Rhodium; Iridium; Palladium; Platinum

1. Introduction and scope

Fluorine forms the strongest single bond to carbon; adding the small size and high electronegativity of this element, the combination give rise to the unusual properties associated with fluorinated organic compounds [1].

The introduction of fluorinated groups into organic molecules can cause a dramatic change in their physical properties, chemical reactivity and physiological activity [2] and therefore it is not surprising that, for example, the number of fluorine-containing drugs has increased dramatically in recent years and its application in agrochemical and veterinarian products follow a similar pattern. At present, up to 30–40% of agrochemicals and 20–30% of pharmaceuticals contain at least one fluorine atom [3].

The chemical inertness and high thermal stability of fluorocarbons have made them useful in a variety of exceptional applications from frying pan coating [4] to artificial blood but, at the same time have increased public concerns over their ecological impact particularly on the upper atmosphere. The stability imparted by the C–F bonds leads to the long atmospheric lifetimes of chlorofluorocarbons (CFCs); saturated perfluorocarbons (PFCs) are even more stable, with CF_4 having an estimated stratospheric lifetime of more than 10,000 years [5].

This chemical inertness makes the chemistry of fluorocarbons a specialized field, an area of research that has attracted

* Tel.: +52 5 6223724; fax: +52 5 6223724.
E-mail address: torrens@servidor.unam.mx.

0010-8545/$ – see front matter © 2005 Elsevier B.V. All rights reserved.
doi:10.1016/j.ccr.2005.01.025

the attention of inorganic and organometallic chemists and new routes to transform these bonds are the subject of many investigations. The chemical and intellectual challenges of C–F bond activation rival those of C–H activation in hydrocarbons.

Transition metals are employed as homogeneous catalysts to modify hydrocarbons in several industrial processes such as olefin hydrogenations, hydroformylations and polymerizations. Analogous processes do not presently exist for fluorocarbons but it has become evident that interaction of fluorocarbons with metal centers may ultimately lead to the cleavage of the robust carbon–fluorine bonds.

A variety of C–F activation reactions that employ metal complexes, require comparatively mild conditions, are selective, and afford isolable products are now known and catalytic systems have been achieved.

Several reviews, focused on the functionalization of C–F bonds, provide a solid background. The activation of unreactive bonds has been reviewed by Murai [6]; Braun and Perutz [7] have summarized their search for routes to fluorinated organic derivatives by nickel-mediated C–F activation of heteroaromatics. The coordination chemistry of the C–F unit in fluorocarbons was reviewed by Plenio [8], whereas Roesky and co-workers [9] have reviewed the compounds containing carbon–metal–fluorine fragments of the d-block metals. Also relevant to the topic of C–F activation are the reviews of Doherty and Hoffman [10]. Richmond has published a chapter dealing with metal reagents for activation and functionalization of carbon–fluorine bonds [11]. The advances in the reaction chemistry of totally saturated PFCs and CFCs with special focus on the defluorination chemistry were summarized by Saunders in 1996 [12].

The areas dealt with in these reviews and fundamental aspects of fluorine chemistry will be not specifically addressed in this work although theoretical studies which provide insight into the mechanism of these reactions will be summarized at the appropriate entries.

A comprehensive review of C–F bond activation by metals was published by Richmond and co-workers [13] in 1994 and further progress in the field was updated by Crabtree and co-workers [14] in 1997.

We will provide an update on the area of fluorocarbon coordination to platinum group metals by surveying the work reported since the review by Richmond and co-workers [13] in 1994. C–F activation by PGM complexes shall be addressed in the context of each metal separately. The literature up to August 2004 is covered.

2. Ruthenium

Gérard and Eisenstein [15] have investigated by density functional theory (DFT) activation barriers and transition state structures for the insertion of ethylene or fluoroethylene in the Ru–H or Ru–F bond of unsaturated 16-electron pentacoordinated complexes [RuClH(olefin)L_2], [Ru(H)(CO)(olefin)L_2]$^+$ or [RuClF(CH_2=CH_2)L_2], L=PH_3, to give 14-electron tetracoordinated β-agostic alkyl complexes. Low activation barriers have been found in the case of insertion of ethylene or fluoroethylene in the Ru–H bound of the metal fragment [RuHClL_2]. Using the olefin complexes as energy references, substitution of an H by an F on ethylene stabilizes the alkyl complex only if F is at the α-position; a destabilization is observed if F is on the β-position of the alkyl group. The energy barriers for insertion follow the relative energies of the alkyl products: the energy barrier is the lowest for insertion of fluoroethylene with F going to the α-carbon of the alkyl chain, the energy barrier is the highest for insertion of fluoroethylene with F going on the β-carbon and the energy barrier in the case of ethylene is intermediate. These features follow the Hammond postulate. In contrast, high-energy barriers and unusual geometrical features with non-monotonic variation of bond lengths along the reaction path have been found with a π-acceptor ligand CO on Ru. The energy barrier for insertion of ethylene in the Ru–H bond is over 15 kcal mol^{-1} higher for [Ru(H)(CO)(CH_2=CH_2)L_2]$^+$ than for [RuH(Cl)(CH_2=CH_2)L_2]. The energy barrier for the insertion in the Ru–F bond of [RuF(Cl)(CH_2=CH_2)L_2] has also a very high barrier. This later result generalizes those found on the high barriers associated with C–F α-migration [16], C–F oxidative addition [17] and migration in the proximity of F [18]. Using an energy decomposition based on a thermodynamic cycle, it is shown that the high energy barrier for insertion of ethylene in the Ru–H bond of [Ru(H)(CO)(CH_2=CH_2)L_2]$^+$ is due to the rigidity of the metal fragment [Ru(H)(CO)L_2]$^+$ which energetically disfavors the change of coordination necessary to go from reactant to product. In the case of ethylene insertion in the Ru–F bond, the high activation barrier is associated with the presence of an F lone pair coplanar with the ethylene ligand which creates some destabilizing interaction with the π-orbital of ethylene.

Perutz and co-workers [19,20] have reported that *cis*-[Ru(H)$_2$(dmpe)$_2$] (dmpe = $Me_2PCH_2CH_2PMe_2$) reacts at −78 °C with hexafluorobenzene to generate the pentafluorophenyl hydride complex *trans*-[Ru(H)(C_6F_5)(dmpe)$_2$], *trans*-[RuH(FHF)(dmpe)$_2$] which is a rare example of a complex containing M–H and M–F bonds, and is unique in the octahedral stereochemistry of hydride *trans* to fluorine [10] and [Ru(H)(dmpe)$_2$](HF_2). As shown in Fig. 1, reaction also takes place with other fluorinated arenes to yield products from C–F insertion exclusively.

Although the proposed mechanism was that of an electron-transfer process involving a caged radical pair, recent studies by Jones and co-workers [21] have found strong evidence to suggest that an anionic nucleophilic mechanism should be considered as an alternative.

A sequence for the formation of the bifluoride hydride that involves an intermediate dihydrogen hydride complex is shown in Eqs. (1) and (2) where [Ru] = [Ru(dmpe)$_2$]:

$$[Ru]H_2 + HF \rightarrow [Ru](\eta^2\text{-}H_2)H^+F^- \quad (1)$$

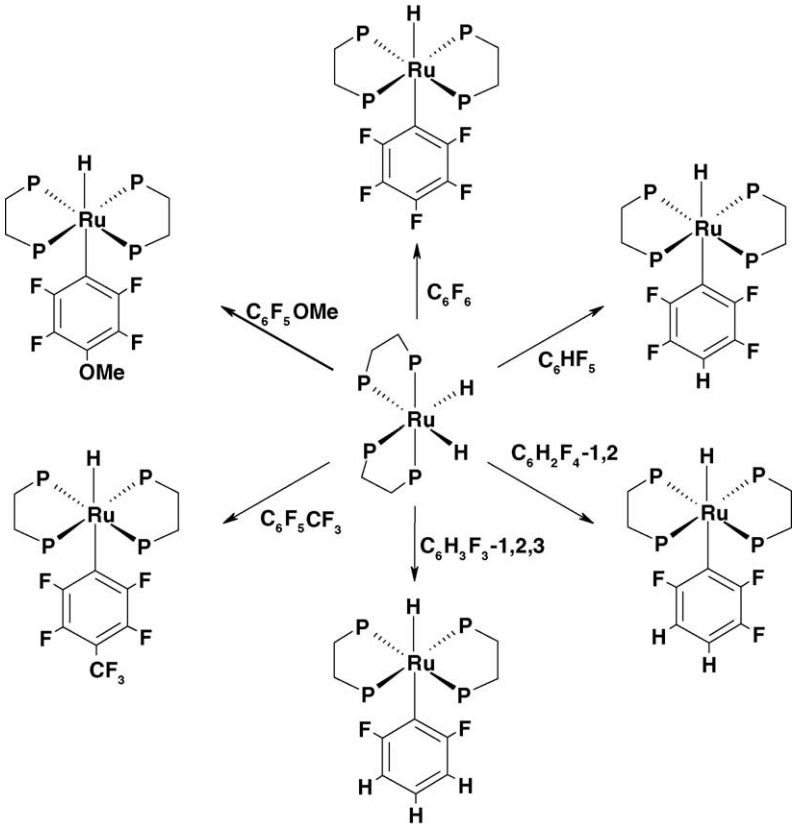

Fig. 1. Reactions of *cis*-[Ru(H)$_2$(dmpe)$_2$] with fluoroaromatic compounds [19].

$$[Ru](\eta^2\text{-}H_2)H^+F^- + HF \rightarrow [Ru](H)(HF_2) + H_2 \quad (2)$$

Extending these results, Whittlesey and co-workers [22] have found that the reaction of $(CF_3)_2C{=}C(F)CF_2CF_3$ or $CF_3CF{=}CF_2$ with *cis*-[Ru(H)$_2$(dmpe)$_2$] affords the bifluoride fluoride complex *cis*-[RuF(FHF)(dmpe)$_2$], in preference to the hydride product, whereas reaction with *cis*-[Ru(H)$_2$(dcpe)$_2$] [dcpe = $(C_6H_{11})_2PCH_2CH_2P(C_6H_{11})_2$] yields the 16-electron hydride species $[Ru(H)(dcpe)_2]^+$ with $[(CF_3)_2C{=}C(O)CF_2CF_3]^-$ as the anion.

Caulton and co-workers [23] have explored the chemistry of [RuH(CO)(P^{t}Bu$_2$Me)$_2$]B(3,5-C$_6$H$_3$(CF$_3$)$_2$)$_4$ obtained according to Fig. 2 [24,25].

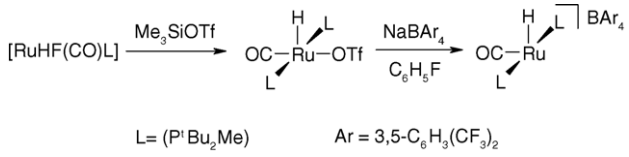

Fig. 2. Synthesis of [RuH(CO)(P^{t}Bu$_2$Me)$_2$]B(3,5-C$_6$H$_3$(CF$_3$)$_2$)$_4$ [24,25].

With $[RuH(CO)(P^tBu_2Me)_2]^+$ excess $CH_2{=}CHF$ forms, at −70 °C, a 1:1 adduct, $[RuH(\eta^2\text{-}CH_2{=}CHF)(CO)(P^tBu_2Me)_2]^+$, which is a chiral complex. The two phosphines are inequivalent, and the ^{31}P-{^{1}H} NMR spectrum shows an AB pattern with P–P coupling constant smaller than that found in $[RuH(\eta^2\text{-}CH_2{=}CHCH_3)(CO)(P^tBu_2Me)_2]^+$ (140 Hz versus 165 Hz for the propylene adduct). The ^{19}F NMR signal of the coordinated $CH_2{=}CHF$ has moved strongly upfield (−150 ppm) compared to that of free vinyl fluoride (−115 ppm). A low-field hydride signal (−3.1 ppm) reveals it is *trans* to the coordinated vinyl fluoride. Upon warming the solution to room temperature, free ethylene is formed along with at least seven phosphine-containing products (Fig. 3). Some of these are doublets by ^{31}P-{^{1}H} NMR, with

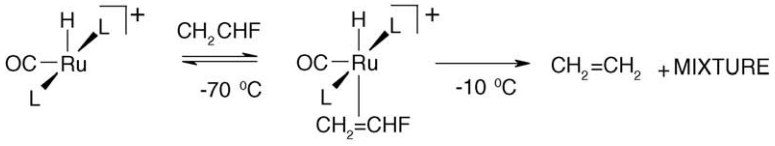

Fig. 3. Formation of $CH_2{=}CH_2$ from $CH_2{=}CHF$ [23].

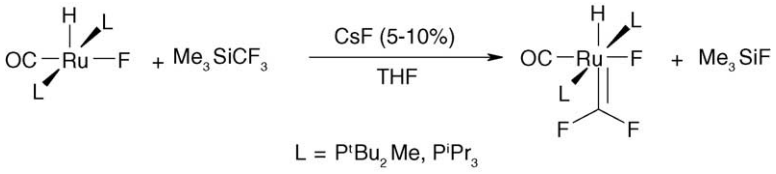

Fig. 4. Formation of [Ru(H)(F)(=CF_2)(CO)L_2] [26].

coupling constants around 20 Hz, presumably to fluorine on Ru.

Caulton and co-workers have found [26] that in the presence of a catalytic amount of F^- (CsF), Me_3SiRf (Rf = CF_3 and C_6F_5) exchanges Rf with fluoride of the 16-electron complexes [Ru(H)(F)(CO)L_2] (L = P^iPr_3, P^tBu_2Me) to give Me_3Si–F and the unsaturated pentafluorophenyl complexes, [RuH(C_6F_5)(CO)L_2], or (when Rf = CF_3) saturated fluorocarbene complexes, [Ru(H)(F)(=CF_2)(CO)L_2], via α-fluorine migration (Fig. 4).

X-ray crystal structure and solution ^{19}F NMR studies reveal that, in the ground state, the three atoms of the CF_2 group lie in a plane perpendicular to the P–Ru–P axis so that the π-back-donation is maximized and the carbene substituents are inequivalent. Having hydride *trans* to the CF_2 ligand, [M(H)(F)(CF_2)(CO)L_2] is a kinetic product, which converts to a thermodynamic isomer. For Ru, the final product is a 16-electron complex, [RuF(CF_2H)(CO)L_2], formed by combination of CF_2 and hydride. For Os, the product is an 18-electron complex, [OsF_2(=CFH)(CO)L_2], resulting from exchange of one carbene fluoride with the hydride. The distinct difference between Os and Ru demonstrates the principle that third-row transition metals show a pronounced tendency toward a higher oxidation state. The isomerization mechanism involves phosphine dissociation as a slow step. Coordinatively saturated [Ru(H)(F)(CF_2)(CO)L_2] reacts with CO within the time of mixing to give the F and CF_2 recombination product, [RuH(CF_3)$(CO)_2L_2$]. This unexpectedly fast carbonylation reaction, as well as ^{19}F spin saturation transfer experiments, reveals the existence of a fast α-F migration equilibrium between [Ru(H)(F)(CF_2)(CO)L_2] and [RuH(CF_3)(CO)L_2] in solution. In sharp contrast, the Os analogue does not have such a fast equilibrium, and therefore it does not react with CO at room temperature.

At higher temperature, reaction occurs forming the hydride and fluoride exchanged product, [Os(CHF_2)(F)$(CO)_2L_2$].

The contrasting behavior of Ru versus Os regarding stability of fluoroalkyl and fluorocarbene is discussed on the basis of theoretical calculations.

The calculated energies of the various products (Fig. 5) reveal some insights, with the proviso that, by studying simultaneously two metals from the same periodic group, one learns by *comparison*, with the following conclusions:

(1) The reaction of [M(H)(F)(CO)$(PH_3)_2$] M = Ru, Os with H_3Si–CF_3 is calculated to be approximately thermoneutral (4 kcal mol^{-1}) for both M = Ru and Os. This shows that, despite the very strong Si–F bond which is formed, the reactants have comparable stabilities. This suggests that the M–F bond, while synthetically very useful, is itself quite strong.
(2) The (experimentally unobserved) [M(H)(CF_3)(CO)$(PH_3)_2$] species show a structure which presages an unexpected feature of the chemistry reported here: C–F cleavage. The α-agostic F species is a minimum, and its geometry can lead easily only to a product with the CF_2 carbene ligand *trans* to H, where subsequent combination of these ligands is unfavorable.
(3) The full cleavage of the C–F bond, to form M3 from M2, is much more favorable for M = Os (−16 kcal mol^{-1}) than for Ru (thermoneutral). This is in agreement with

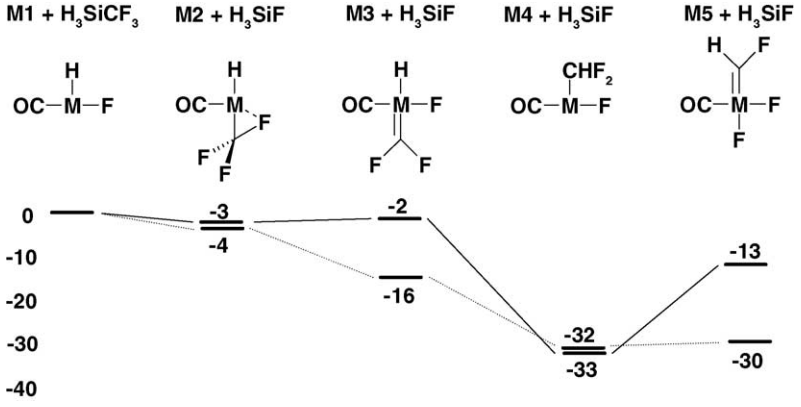

Fig. 5. Calculated energies of the structures shown – optimized – comparing M = Ru (solid lines) to M = Os (dashed lines). For simplicity, PH_3 ligands are omitted from the drawings [26].

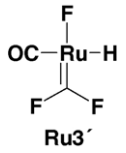

Fig. 6. Isomer *trans* F-(=CF_2) of [Ru(H)(F)(=CF_2)(CO)(PH_3)$_2$]. For simplicity, PH_3 ligands are omitted from the drawings [26].

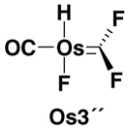

Fig. 7. Isomer *trans* CO-(=CF_2) of [Os(H)(F)(=CF_2)(CO)(PH_3)$_2$]. For simplicity, PH_3 ligands are omitted from the drawings [26].

the experimental fact that Ru3 is detectably in equilibrium with a CF_3 isomer at 60 °C, while this is not the case for Os3. Osmium thus shows a greater preference than ruthenium for being saturated and having more π-acid ligands (i.e., to be more oxidized).

(4) Isomer Ru3′ (Fig. 6), which may be relevant to finally forming the CHF_2 ligand (H has migrated "toward" the carbene), is only 1 kcal mol^{-1} higher in energy than Ru3. This shows that H has an energetically comparable effect whether it is *trans* to CO or to CF_2.

(5) Isomer Os3″ (Fig. 7), where the carbene has migrated "toward" H, is 6 kcal mol^{-1} less stable than Os3. This must be attributed to competition between the two π-acid ligands CO and CF_2 for back-bonding and the decreased push/pull interaction between F and CO in Os3″.

(6) The transformation from M3 to M4 is very favorable for both metals, although much more so for Ru than for Os. This metal dependence of ΔE_{3-4} can be attributed to the same effects cited above: a greater preference for saturation, and the greater reducing power of the 5d metal. Consistent with this logic, the isomerization of Os4 Os5 is thermoneutral, while it is unfavorable by 20 kcal mol^{-1} for Ru. Thus, for Ru, any benefit from achieving an 18-valence electron count must be offset by the diminished reducing power of this 4d metal: it is less able than osmium to tolerate the additional π-acid ligand CF_2.

In broad strokes, then, the calculations agree with experiment for ruthenium, and they give a quantitative measure of the stability of isomers, both observed and unobserved.

3. Osmium

Caulton and co-workers [26] have carried out density functional theory (DFT) calculations to study the contrasting behavior of Ru versus Os regarding the stability of fluoroalkyl and fluorocarbene complexes. This work is summarized in Section 2.

In the solid phase [Os(SC_6F_5)$_3$(PMe_2Ph)$_2$] exhibits an interaction of an *ortho*-fluorine of one of the SC_6F_5 ligands with the metal to create an S–F five membered chelate ligand, thus achieving six coordination in an approximately octahedral arrangement [27,28].

Thermolysis of [Os(SC_6F_5)$_3$(PMe_2Ph)$_2$] in refluxing toluene affords [Os(SC_6F_5)$_2$(*o*-$S_2C_6F_4$)(PMe_2Ph)] and [Os(C_6F_5)$_2$(*o*-$S_2C_6F_4$)(PMe_2Ph)$_2$] a rare example of a C–F activation from perfluorothiolate ligands to afford 1,2-dithiolate complexes.

To rationalize the outcome of this reaction, cleavage of an *ortho*-C–F bond at a thiolate ligand, intermolecular transfer of a sulfur atom and dissociation of a phosphine molecule have to be considered. Formation of [Os(SC_6F_5)$_2$(*o*-$S_2C_6F_5$)(PMe_2Ph)] and [Os(C_6F_5)$_2$(*o*-$S_2C_6F_4$)(PMe_2Ph)$_2$] also require oxidation of the metal centers.

An Ar–F–Os interaction is expected to induce an activated *ortho*-C–F bond bearing an electrophilic carbon atom. Therefore the *ortho*-carbon atom of complex [Os(SC_6F_5)$_3$(PMe_2Ph)$_2$] can be envisaged as the center of a nucleophilic attack by a thiolate-sulfur atom.

Esteruelas and co-workers [29] have demonstrated that the hexahydride–osmium complex [OsH_6(P^iPr_3)$_2$] is capable of activating *ortho*-C–F bonds of fluorinated aromatic ketones. Thus, the reactions of this complex with pentafluoroacetophenone, decafluorobenzophenone and 2,6-difluoroacetophenone give [OsH_3($C_6F_4C(O)R$)(P^iPr_3)$_2$] (R = CH_3, C_6F_5) and [OsH_3($C_6H_3FC(O)CH_3$)(P^iPr_3)$_2$] (Fig. 8).

The structure of [OsH_3($C_6F_4C(O)CH_3$)(P^iPr_3)$_2$] has been determined by X-ray diffraction. The geometry around the osmium atom can be described as a distorted pentagonal bipyramid with the phosphine ligands occupying axial positions.

Complexes [OsH_3($C_6F_4C(O)CH_3$)($PiPr_3$)$_2$] and [OsH_3($C_6H_3FC(O)CH_3$)(P^iPr_3)$_2$] can also be obtained by reaction of [OsH_6(P^iPr_3)$_2$] with 2,3,4,5-tetrafluoroacetophenone and 2-fluoroacetophenone, respectively. This selective C–H activation of the *ortho*-C–H bond of the above-mentioned ketones is in contrast with the selective C–F activation observed for the reaction of [OsH_6(P^iPr_3)$_2$] with 2,3,4,5,6-pentafluorobenzophenone, which affords [OsH_3($C_6F_4C(O)C_6H_5$)(P^iPr_3)$_2$]. The structure of [OsH_3($C_6F_4C(O)C_6H_5$)(P^iPr_3)$_2$] has also been determined by X-ray diffraction.

Density functional theory (DFT) calculations suggest that, in agreement with the C–F activation of 2,3,4,5,6-pentafluorobenzophenone, in aromatic ketones the C–F activation is much more favored than the C–H activation, from a thermodynamic point of view. So, the preferred C–H activation in 2-fluoroacethophenone and 2,3,4,5-tetrafluoroacetophenone appears to have kinetic origin, which could be, in part, related with the preferred *anti* arrangement of the F–C–C–C=O unit of the starting ketones.

In conclusion, complex [OsH_6(P^iPr_3)$_2$] activates *ortho*-C–H and *ortho*-C–F bonds of aromatic ketones. The

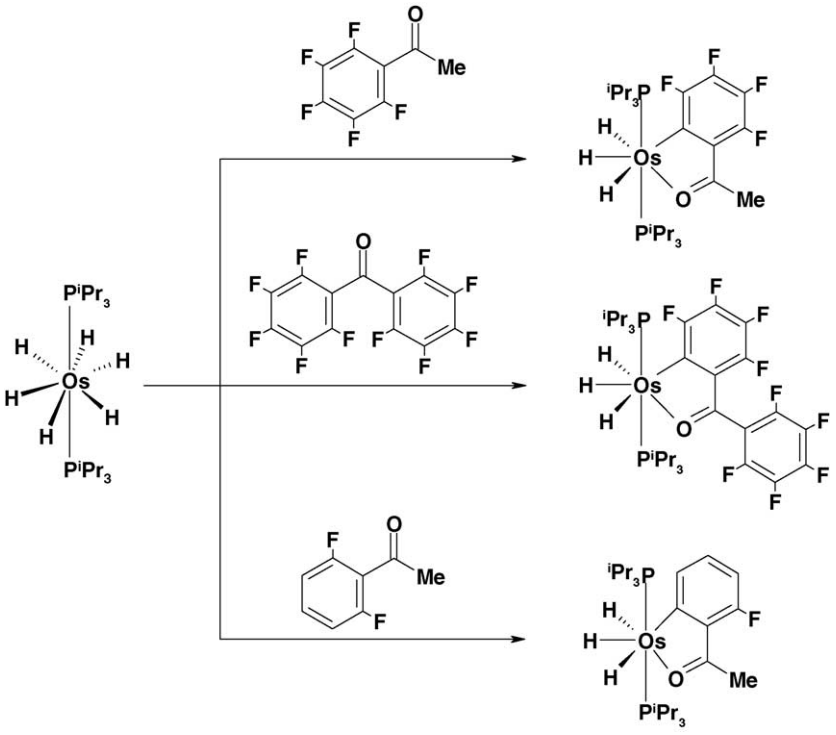

Fig. 8. Reactions of $[OsH_6(P^iPr_3)_2]$ with aromatic ketones [29].

ortho-C–H activation is preferred over the *ortho*-C–F activation in ketones containing only one aromatic ring, whereas the *ortho*-C–F activation is preferred over the *ortho*-C–H activation in 2,3,4,5,6-pentafluorobenzophenone.

Caulton and co-workers [30] have studied the vinyl C–F cleavage by $[Os(H)_3Cl(P^iPr_3)_2]$. This osmium complex reacts at 20 °C with vinyl fluoride in the time of mixing to produce $[OsHFCl(\equiv CCH_3)(P^iPr_3)_2]$ and H_2. In a competitive reaction, the liberated H_2 converts vinyl fluoride to C_2H_4 and HF in a reaction catalyzed by $[Os(H)_3Cl(P^iPr_3)_2]$. A variable-temperature NMR study reveals these reactions proceed through the common intermediate $[OsHCl(H_2)(H_2C{=}CHF)(P^iPr_3)_2]$, via $[OsClF(=CHMe)(P^iPr_3)_2]$ and $[OsHCl(H_2)(C_2H_4)(P^iPr_3)_2]$, all of which are detected.

Density functional theory, DFT(B3PW91), calculations of the potential energy and free energy at 298 K of possible intermediates show the importance of entropy to account for their thermodynamic accessibility. Calculations of unimolecular C–F cleavage of coordinated C_2H_3F confirm the high activation energy of this process. Catalysis by HF is thus suggested to account for the fast observed reactions, and scavenging of HF with NEt_3 changes the product to exclusively $[Os(H)_2Cl(CCH_3)(PH_3)_2]$. The analogous reaction of $[Os(H)_3Cl(PH_3)_2]$ with $H_2C{=}CF_2$ produces exclusively $[OsHFCl(=CCH_3)(PH_3)_2]$ and HF, and the latter is again suggested to catalyze C–F scission via the observed intermediates $[Os(H)_2Cl(CF_2CH_3)(PH_3)_2]$ and $[OsHCl(=CFMe)(PH_3)_2]$.

4. Rhodium

Su and Chu [31] reported in 1997 one of the first theoretical studies of C–F activation. The oxidative addition of the F–CH_3 bond to coordinatively unsaturated *trans*-$[M(X)(PH_3)_2]$ and $[M(PH_3)_3]$ (M = Rh, Ir; X = CH_3, H, Cl) was investigated by DFT. All of the stationary points were determined at the B3LYP/LANL2DZ level. A configuration mixing model based on the theory of Pross and Shaik was used to develop an explanation for the barrier height as well as the reaction enthalpy. The theoretical observations suggest that the singlet–triplet splitting ($\Delta E_{st} = \Delta_{triplet} - \Delta_{singlet}$) of the $[M(PH_3)_3]$ species can be used as a basis to predict its reaction activity for oxidative additions, i.e., the smaller the ΔE_{st} of ML_3, the lower the barrier height and the larger the exothermicity, in turn, the faster the oxidative addition reaction.

The potential energy profiles are summarized in Fig. 9. Four interesting conclusions can be drawn from this figure.

First, for the same metal center, the better π-donor the ligand X, the lower the activation energy and the larger the exothermicity for the oxidative addition of F–CH_3 to $[M(X)(PH_3)_2]$ complexes (left to right in Fig. 9). For instance, since the Cl ligand is a stronger π-donor than CH_3 and H, the barrier height for F–CH_3 activation with M = Rh increases in the order $[Rh(Cl)(PH_3)_2]$ (9.6 kcal mol^{-1}) < $[Rh(H)(PH_3)_2]$ (17 kcal mol^{-1}) < $[Rh(CH_3)(PH_3)_2]$ (18 kcal mol^{-1}) and, for M = Ir, $[Ir(Cl)(PH_3)_2]$ (4.6 kcal mol^{-1}) < $[Ir(H)(PH_3)_2]$ (15 kcal mol^{-1}) ∼ $[Ir(CH_3)(PH_3)_2]$ (15 kcal mol^{-1}). It is

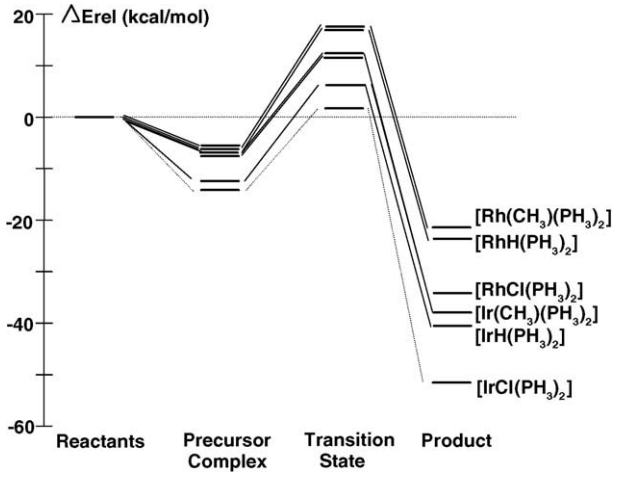

Fig. 9. Potential energy surfaces for the activation of the F–CH_3 bond by *trans*-[M(X)$(PH_3)_2$] (M = Rh, Ir; X = CH_3, H, Cl) [31].

noteworthy that the activation barriers for the Ir reactions are smaller than those for their Rh analogues.

Second, all of the oxidative addition reactions are thermodynamically exothermic. The order of exothermicity follows the same trend as the activation energy: [Rh(Cl)$(PH_3)_2$] (-34 kcal mol^{-1}) < [Rh(H)$(PH_3)_2$] (-26 kcal mol^{-1}) < [Rh(CH_3)$(PH_3)_2$] (-23 kcal mol^{-1}) and [Ir(Cl)$(PH_3)_2$] (-51 kcal mol^{-1}) < [Ir(H)$(PH_3)_2$] (-41 kcal/mol) < [Ir(CH_3)$(PH_3)_2$] (-38 kcal mol^{-1}). Again, the Ir reactions are more exothermic than their Rh counterparts.

Third, the model calculations also suggest that oxidative additions involving a third-row transition metal (such as Ir) should be preferable to those of a second-row transition metal (such as Rh) since it is demonstrated not only that the former are thermodynamically more favorable but also that the kinetic barriers associated with them are typically small. On the other hand, the reductive elimination (right to left in Fig. 9) of the second-row metal is more favorable than that of the third-row homologue.

Fourth, the transition state studies based on the model systems Su and Chu have used strongly suggest that radical intermediates should not be involved in C–F activation reactions for the 14-electron d^8 [M$(PH_3)_3$] cases. Moreover, the energetics shown in Fig. 9 indicate that the model reactions actually have low activation energies for activation of the C–F bond by coordinatively unsaturated [M(X)$(PH_3)_2$] complexes. For example, the activation barrier relative to the corresponding reactants for F–CH_3 insertion to [Ir(Cl)$(PH_3)_2$] was calculated at the B3LYP/LANL2DZ level to be 4.6 kcal mol^{-1} and the activation energies for the whole reactions are about 18 kcal mol^{-1}. It is estimated that these barriers will be greatly improved with more complete calculations. Additionally, the overall energy of this reaction is exothermic by 51 kcal mol^{-1}. In any event, the 14-electron [Ir(Cl)$(PH_3)_2$] complex is a potential model for oxidative addition of saturated C–F bonds kinetically as well as thermodynamically. As there are no relevant experimental and theoretical data on such systems, the above results are predictions.

Eisenstein and co-workers [32] have carried out quantum calculations with the density functional theory DFT (B3LYP) to compare the reactivity of aryl–H and aryl–F bonds toward oxidative addition and to understand the high degree of inertness of the latter. The thermodynamic energy patterns for oxidative addition of 1,4-difluorobenzene toward two very different Os and Rh metal fragments have been examined. In one of them the final product of oxidative addition could be a 16-electron unsaturated complex of the type [Os(H)(CO)($C_6F_2H_3$)$(PH_3)_2$] and/or [Os(F)(CO)(C_6FH_4)$(PH_3)_2$]. In the other system the final product of oxidative addition could be an 18-electron saturated complex [Rh(η^5-C_5H_5)(H)($C_6F_2H_3$)(PH_3)] or [Rh(η^5-C_5H_5)(F)($C_6F_2H_3$)(PH_3)]. These two systems are models for experimental complexes which prefer the C–H to the C–F oxidative addition. The calculations reveal that, for both systems, the C–F oxidative addition is thermodynamically preferred, especially in the 16-electron case. The activation energy has been determined in the case of Rh, and it is shown that the activation energy for C–F activation is considerably higher than that for C–H activation. This clearly shows that the inertness of the C–F bond has a kinetic origin.

Aizenberg and Milstein [33] have found that aromatic C–F bond can be cleaved by rhodium complexes even at room temperature and that this reaction can be elaborated into homogeneous catalysis involving C–F bonds. These catalytic cycles, which were designed by a combination of individual stoichiometric reactions exhibit high selectivity (see Fig. 10).

The Rh(I) silyl complex [Rh($SiMe_2Ph$)(PMe_3)$_3$], synthesized from [RhCl(PMe_3)$_3$] and $LiSiMe_2Ph$, Eq. (3), reacts quantitatively with C_6F_6 at room temperature.

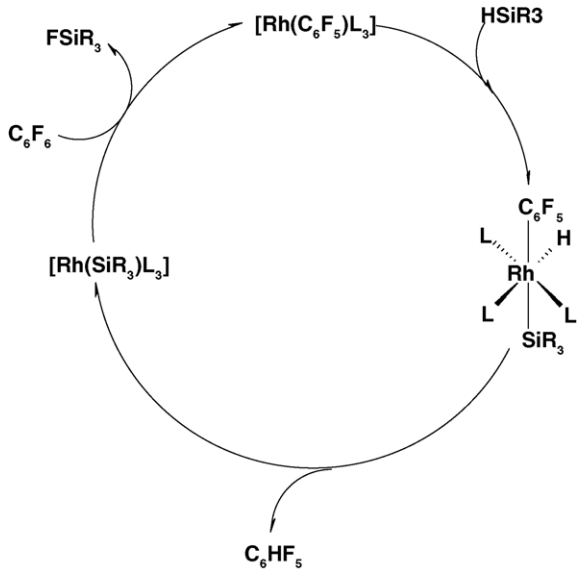

Fig. 10. Catalytic cycle converting C_6F_6 into C_6HF_5 by [Rh(C_6F_5)L_3] [33].

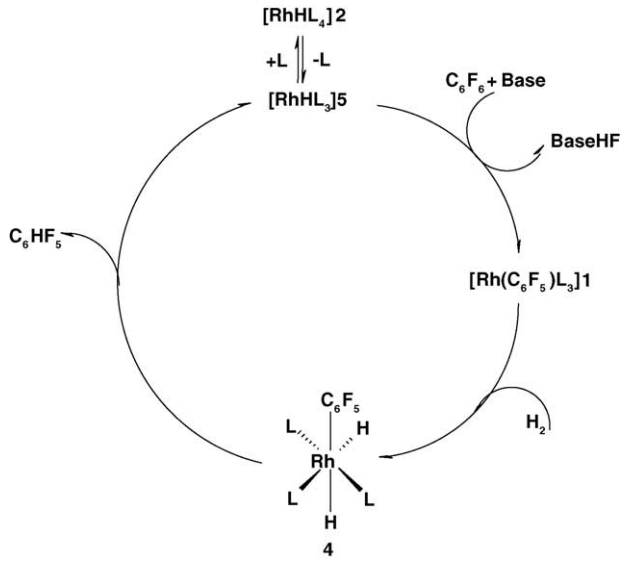

Fig. 11. Catalytic cycle for the hydrogenolysis of C_6F_6 in the presence of PMe_3 complexes of rhodium [34].

$$[Rh(SiR_3)(PMe_3)_3] + C_6F_6 \rightarrow [Rh(C_6F_5)(PMe_3)_3] + R_3 \quad (SiFR_3 = Me_2Ph, Ph_3) \qquad (3)$$

Heating $[RhC_6F_5(PMe_3)_3]$ or $[RhH(PMe_3)_4]$ at 95–100 °C in C_6F_6 or C_6HF_5 in the presence of a base (Et_3N or a mixture of Et_3N and K_2CO_3) under 85 psi of hydrogen leads to the substitution of F by H and capturing of the released HF by the base (Fig. 11) [34].

Except for the C–F activation step all other reactions depicted in Fig. 11, namely 1–4 and 4–5, are normal H–H oxidative addition and C–H reductive elimination. As for the transformation 5–1, which has been demonstrated to occur readily, and which is the central step in the cycle, it was believed that it proceeds via electron transfer from the complex to the substrate with subsequent release of fluoride ion but later evidence [21] points to an anionic nucleophilic mechanism.

The cycle with C_6HF_5 as a substrate is completely analogous to the one depicted in Fig. 11. The difference between the two is the participation of the analogs of 1 and 4 which have C_6HF_4 rather than C_6F_5 group bound to the rhodium center and correspondingly produce $C_6H_2F_4$. In summary, Milstein and Aizenberg have demonstrated that trimethylphosphine complexes of rhodium efficiently catalyze homogeneous hydrogenolysis of the strong C–F bonds of polyfluorinated benzenes under mild conditions in the presence of a base which is a rare case of homogeneous transition-metal-catalyzed C–F activation. In addition, they also had shown that the reaction exhibits chemo- and regioselectivity. The proposed catalytic cycle for the hydrogenolysis involves electron-rich hydrido-rhodium(I) phosphine complexes as the species that induce cleavage of C–F bonds. This implies that other complexes which can serve as a good source of such species are also likely to be active.

Edelbach and Jones [21] found that the complex $[Rh(\eta^5\text{-}C_5Me_5)(H)_2(PMe_3)]$ reacts with C_6F_6, C_6F_5H, $C_{12}F_{10}$ or $C_{10}F_8$ in pyridine or 1:1 pyridine/benzene to give the C–F cleavage products $[Rh(\eta^5\text{-}C_5Me_5)(aryl\text{–}F)H(PMe_3)]$ in high yield (Fig. 12). Kinetic studies reveal that the reaction has autocatalytic character, and fluoride ion is shown to be responsible for the catalysis. The anion $[Rh(\eta^5\text{-}C_5Me_5)H(PMe_3)]^-$ reacts rapidly with $C_{12}F_{10}$ or $C_{10}F_8$ to give the same C–F cleavage products as $[Rh(\eta^5\text{-}C_5Me_5)(H)_2(PMe_3)]$. A mechanism initiated by deprotonation of $[Rh(\eta^5\text{-}C_5Me_5)(H)_2(PMe_3)]$ followed by nucleophilic attack of the resulting anion on the polyfluoroaromatic with subsequent loss of fluoride is proposed. The fluoride ion continues the cycle by deprotonating $[Rh(\eta^5\text{-}C_5Me_5)(H)_2(PMe_3)]$.

Saunders and co-workers [35,36] have studied the reaction between $[\{M(\eta^5\text{-}C_5Me_5)Cl(\mu\text{-}Cl)\}_2]$ (M = Rh or Ir) and $(C_6F_5)_2PCH_2CH_2P(C_6F_5)_2$ dfppe in refluxing benzene yielded the cationic species $[M(\eta^5\text{-}C_5Me_3(CH_2C_6F_4P(C_6F_5)CH_2)_2\text{-}1,3)Cl]^+$ in which two C–F and two C–H bonds have been cleaved and two C–C bonds formed, HF is also produced (Fig. 13). The complexes $[MCl(\eta^5\text{-}C_5Me_5)(C_6F_5)_2PCH_2CH_2P(C_6F_5)_2]BF_4$ (M = Rh or Ir) which have not undergone C–F bond activation were formed by treatment of $[\{M(\eta_5\text{-}C_5Me_5)Cl(\mu\text{-}Cl)\}_2]$ with $NaBF_4$ and dfppe, and have been structurally characterized by X-ray crystallography. Activation of the C–F bonds in these complexes is induced by thermolysis in refluxing ethanol. The reaction between $[\{M(\eta^5\text{-}C_5Me_5)Cl(\mu\text{-}Cl)\}_2]$ (M = Rh or Ir) and dfppe in refluxing ethanol yielded a mixture of the cations $[MCl(\eta^5\text{-}C_5Me_5)(dfppe)]^+$, $[MCl(\eta^5\text{-}C_5Me_5)(C_6F_5)_2PCH_2CH_2P(C_6F_5)_2]^+$ and, where M = Rh, the singly C–F bond-activated species $[Rh(\eta^5\text{-}C_5Me_4(CH_2C_6F_4P(C_6F_5)CH_2)_2)Cl]^+$.

The reaction [37] between $[\{Rh(\eta^5\text{-}C_5Me_4H)Cl(\mu\text{-}Cl)\}_2]$ and $(C_6F_5)_2PCH_2CH_2P(C_6F_5)_2$ proceeds in refluxing benzene via activation of two C–F and C–H bonds and formation of two C–C bonds to yield the chiral cation $[Rh(\eta^5\text{-}C_5HMe_2\text{–}2,4\text{-}[CH_2C_6F_4P(C_6F_5)CH_2]2\text{-}1,3)Cl]^+$, with >90% selectivity.

The reaction [38] between $[\{Rh(\eta^5\text{-}C_5Me_4Et)Cl(\mu\text{-}Cl)\}_2]$ and the diphosphine, $(C_6F_5)_2PCH_2CH_2P(C_6F_5)_2$ (dfppe), proceeded via the activation of two C–F and two C–H bonds and the formation of two C–C bonds to give a mixture of isomers of a salt with formulation "$[Rh(\eta^5\text{-}C_5Me_4Et)Cl((C_6F_5)_2PCH_2CH_2P(C_6F_5)_2)\text{-}2HF]Cl$". Treatment of $[\{Rh(\eta^5\text{-}C_5Me_4Et)Cl(\mu\text{-}Cl)\}_2]$ with NH_4BF_4 followed by dfppe yielded $[Rh(\eta^5\text{-}C_5Me_4Et)Cl((C_6F_5)_2PCH_2CH_2P(C_6F_5)_2)]BF_4$ which, on thermolysis in ethanol underwent C–F and C–H bond activation to yield the tetrafluoroborate salt "$[Rh(\eta^5\text{-}C_5Me_4Et)Cl((C_6F_5)_2PCH_2CH_2P(C_6F_5)_2)\text{-}2HF]BF_4$".

When the reaction between $[\{Rh(\eta^5\text{-}C_5Me_4Et)Cl(\mu\text{-}Cl)\}_2]$ and dfppe was carried out in ethanol, a mixture of $[Rh(\eta^5\text{-}C_5Me_4Et)Cl(dfppe)]BF_4$ and the singly C–F bond-activated complex "$[Rh(\eta^5\text{-}C_5Me_4Et)Cl((C_6F_5)_2$

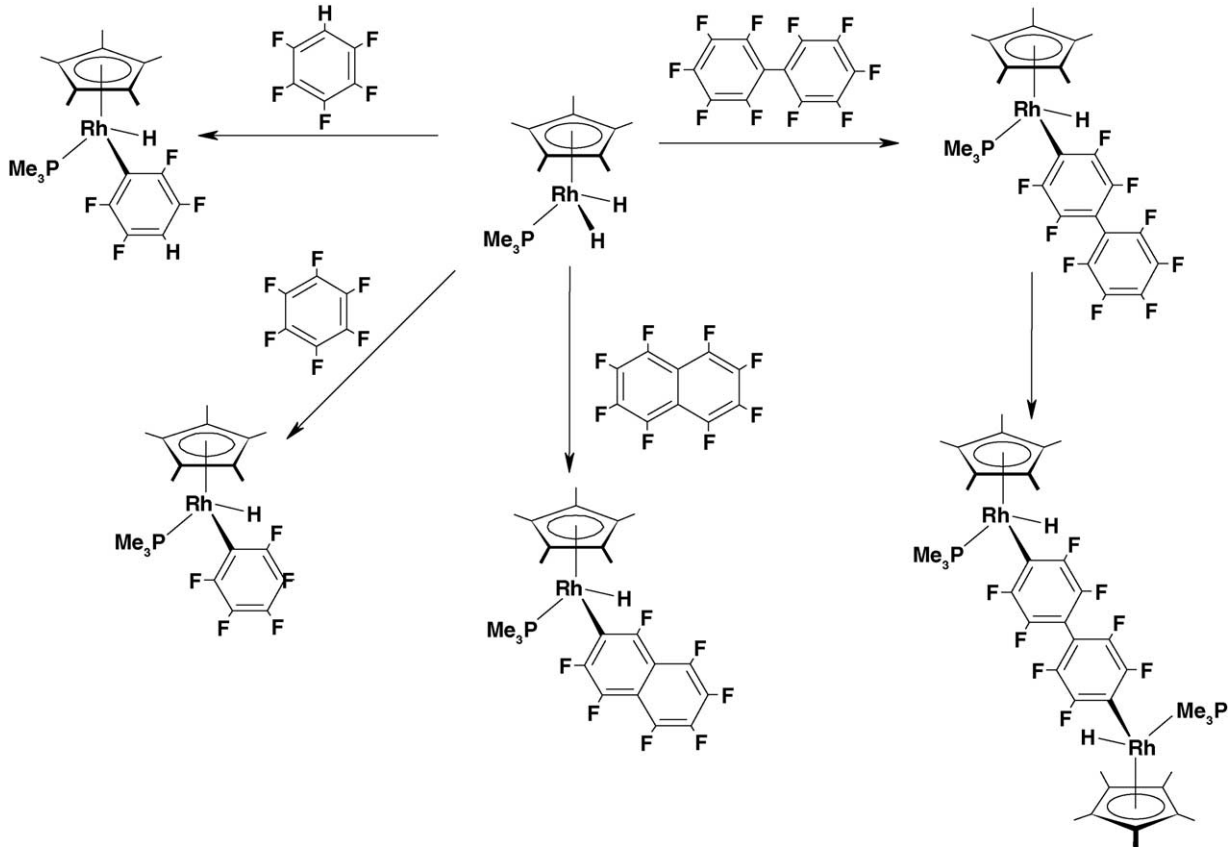

Fig. 12. Reactions of $[Rh(H)_2(\eta^5\text{-}C_5Me_5)(PMe_3)]$ with fluoroaromatic compounds [21].

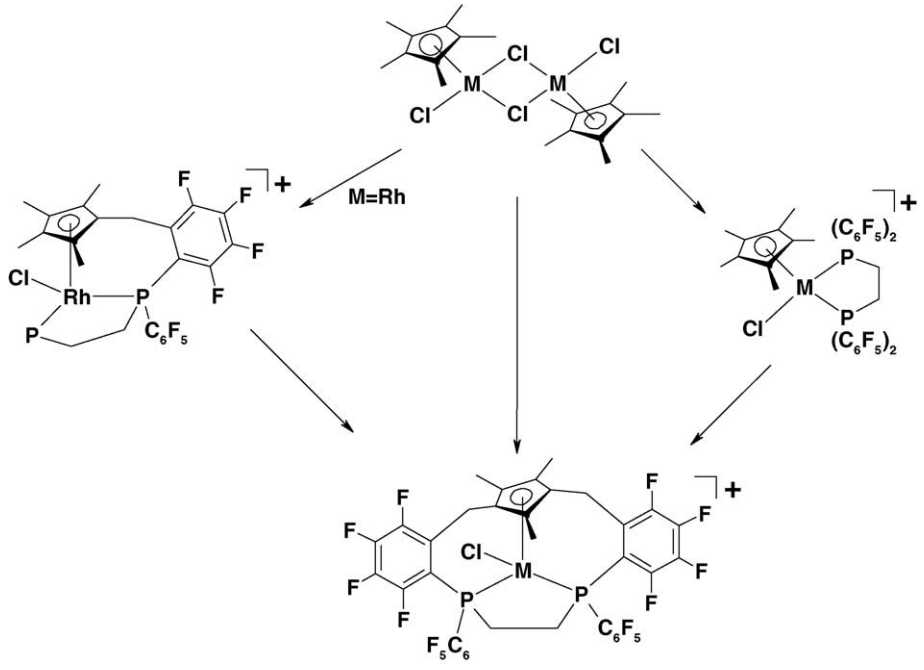

Fig. 13. Reactions of $[\{M(\eta^5\text{-}C_5Me_5)Cl(\mu\text{-}Cl)\}_2]$ M = Rh or Ir and $(C_6F_5)_2PCH_2CH_2P(C_6F_5)_2$ [36].

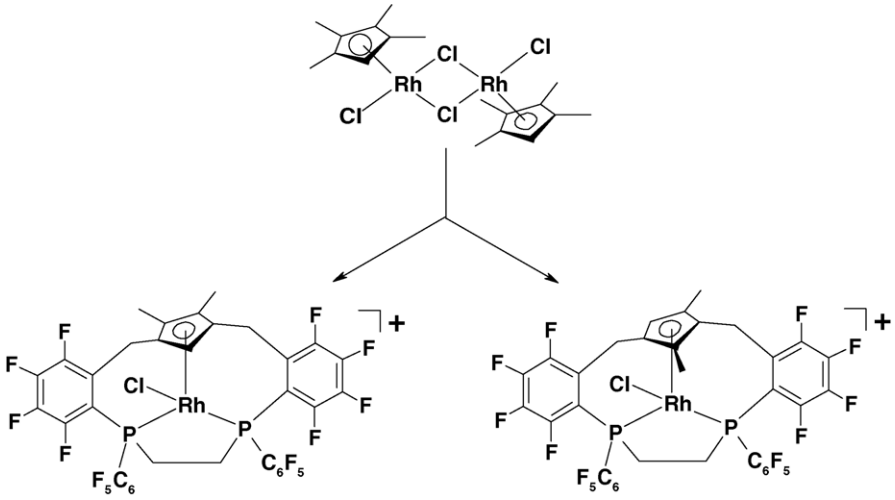

Fig. 14. Reactions of [{Rh(η^5-C_5Me_4H)Cl(μ-Cl)}$_2$] and $(C_6F_5)_2PCH_2CH_2P(C_6F_5)_2$ [37].

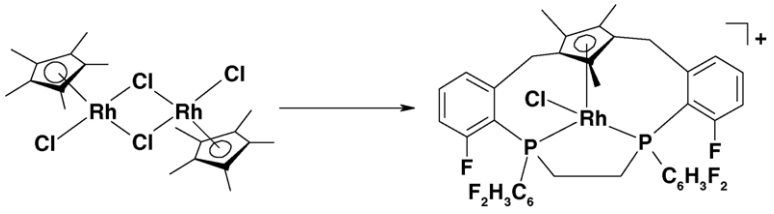

Fig. 15. Reactions of [{Rh(η^5-C_5Me_5)Cl(μ-Cl)}$_2$] and $(C_6H_3F_2\text{-}2,6)_2PCH_2CH_2P(C_6H_3F_2\text{-}2,6)_2$ [39].

$PCH_2CH_2P(C_6F_5)_2$)-HF]BF_4" were obtained after addition of NH_4BF_4.

Extending the work described above [39], the reaction between [{RhCl(μ-Cl)(η^5-C_5Me_5)}$_2$] and the new fluorine-containing diphosphine $(C_6H_3F_2\text{-}2,6)_2PCH_2CH_2P(C_6H_3F_2\text{-}2,6)_2$ in refluxing benzene yielded the cationic species [RhCl(η^5-C_5Me_3(2-$CH_2C_6H_3F$-6)P($C_6H_3F_2$-2,6)CH_2)$_2$-1,3)] which was characterized as the BF_4^- salt. The reaction involved the regiospecific activation of two C–F bonds and two C–H bonds and the formation of two C–C bonds (Figs. 14 and 15).

The rhodium(III) complex [RhCl(μ^5-C_5Me_5)(dfppe)]BF_4, undergoes rapid stepwise intramolecular dehydrofluorinative carbon–carbon coupling on addition of proton sponge to produce [RhCl(η^5,κP,κP-C_5Me_3[$CH_2C_6F_4$–2-P(C_6F_5)CH_2]$_2$-1,3)]BF_4 (Fig. 16) [40].The reaction requires less than the stoichiometric quantity of proton sponge and also occurs on addition of $^nBu_4NF$ or in the presence

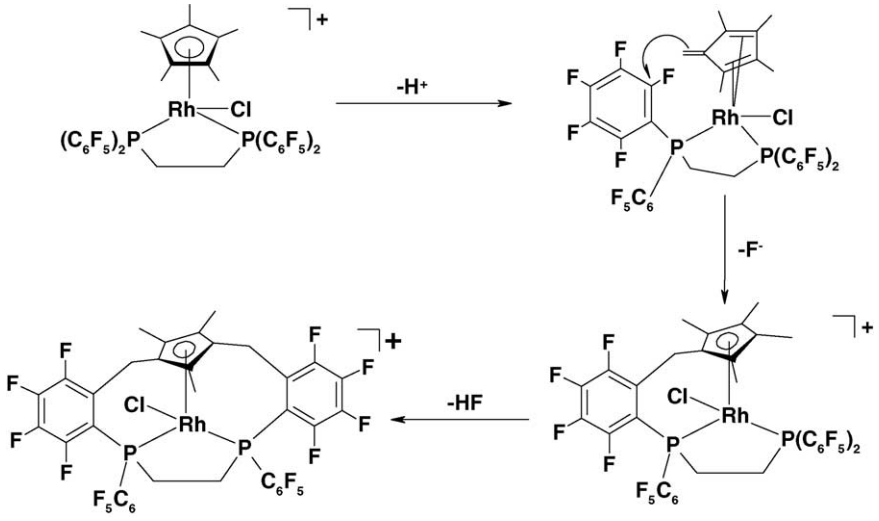

Fig. 16. Stepwise intramolecular dehydrofluorinative carbon–carbon coupling [40].

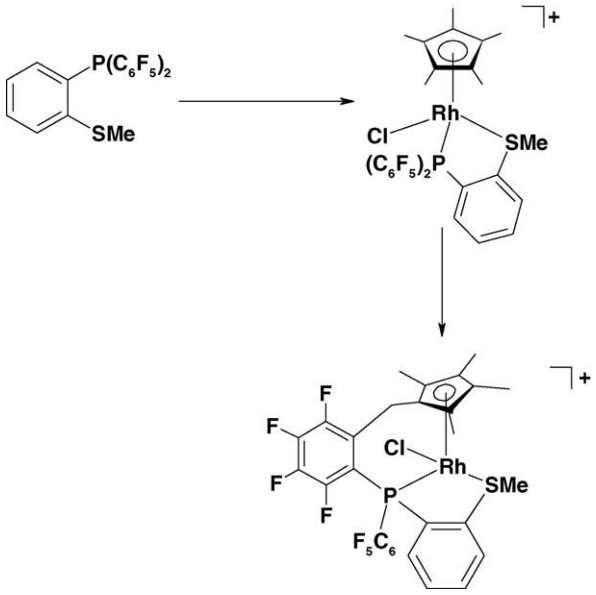

Fig. 17. Synthesis of [RhCl(η^5,κP,κS—$C_5Me_4CH_2C_6F_4P(C_6F_5)C_6H_4SMe$)]$BF_4$ [40].

of polymer-supported fluoride. NMR studies of reactions between a series of complexes and proton sponge have revealed the necessary conditions for intramolecular dehydrofluorinative coupling in pentamethylcyclopentadienyl rhodium(III) phosphine complexes. The complex must be cationic, and the phosphine, which can be either part of a chelating ligand or monodentate need have only one pentafluorophenyl substituent. The reaction is rapid where C_5Me_5 and C_6F_5 are held in close proximity. The compounds [RhCl(η^5-C_5Me_5)((C_6F_5)$_2$$PC_6H_4SMe$-2)]$BF_4$, and the diastereoisomer of [RhCl(η^5-C_5Me_5)((C_6F_5)$PhPC_6H_4SMe$-2)]BF_4, in which C_5Me_5 and C_6F_5 are *cis*, undergo rapid coupling on treatment with proton sponge (Fig. 17). The diastereoisomer of [RhCl(η^5-C_5Me_5)((C_6F_5)$PhPC_6H_4SMe$-2)]BF_4, in which Cp* and C_6F_5 are *trans*, undergoes isomerization at a much slower rate than that of coupling. Cationic complexes of monodentate phosphines, in which there is rotation about the Rh–P bond, undergo coupling on addition of proton sponge, but at a much slower rate than for [RhCl(η^5-C_5Me_5)(dfppe)]BF_4 and [RhCl(η^5-C_5Me_5)((C_6F_5)$PhPC_6H_4SMe$-2)]BF_4. The structures of [RhCl(η^5,κP,κP—$C_5Me_4CH_2C_6F_4$—2-P(C_6F_5)$CH_2CH_2P(C_6F_5)_2$)]BF_4 and [RhCl(η^5,κP,κS-$C_5Me_4CH_2C_6F_4P(C_6F_5)C_6H_4SMe$)]$BF_4$ have been determined by single-crystal X-ray diffraction.

Saunders and co-workers [41] have studied the reaction between [{Rh(μ-Cl)Cl(η^5-C_5Me_5)}$_2$] and the tetrafluoropyridyl-substituted diphosphine $Ph_2PCH_2CH_2PPh$-(C_5F_4N-4) in the presence of BF_4^- yielding racemic diastereoisomers of [RhCl(η^5-C_5Me_5)($Ph_2PCH_2CH_2PPh(C_5F_4N$-4))](BF_4). In the $S_{Rh}R_P$ and $R_{Rh}S_P$ pair of enantiomers the C_5Me_5 and tetrafluoropyridyl groups have a *cis* disposition about the Rh–P bond, and in the $S_{Rh}S_P$ and $R_{Rh}R_P$ pair the groups are *trans*. In situ NMR experiments reveal that the *cis* pair, in which the C_5Me_5 and tetrafluoropyridyl groups are close, underwent rapid dehydrofluorinative C–C coupling to give the respective enantiomers of [RhCl(η^5,κP,κP–$C_5Me_4CH_2$–2-C_5F_3N–4-$PPhCH_2CH_2PPh_2$)]BF_4 (Fig. 18). The *trans* pair did not undergo coupling, but isomerized to the *cis* pair on heating in ethanol. The structure of one enantiomer of [RhCl(η^5,κP,κP–$C_5Me_4CH_2$–2-C_5F_3N–4-$PPhCH_2CH_2PPh_2$)]BF_4 which crystallizes as a conglomerate, has been determined by single-crystal X-ray diffraction.

Perutz and co-workers [42] have shown that irradiation of [Rh(η^5-C_5H_5)(PMe_3)(C_2H_4)] in pentafluoroanisole generates the metallacycle [(η^5-C_5H_5)(PMe_3)$RhCH_2OC_6F_4$];

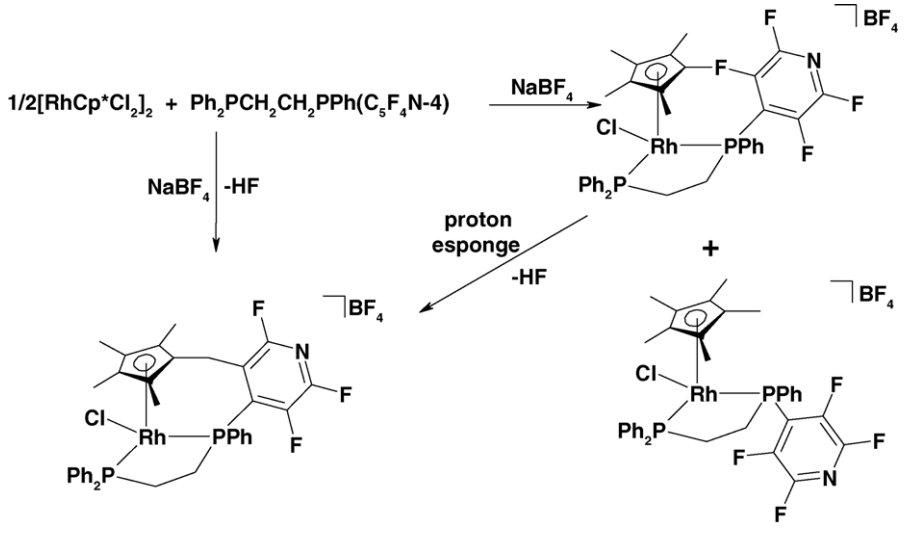

Fig. 18. Synthesis of [RhCl(η^5,κP,κP—$C_5Me_4CH_2$—2-C_5F_3N—4-$PPhCH_2CH_2PPh_2$)]BF_4 [41].

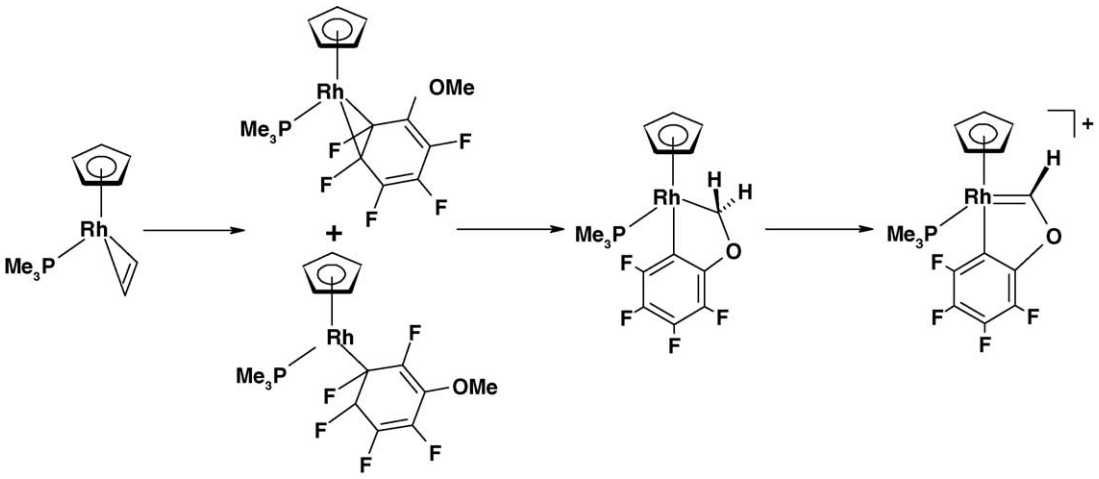

Fig. 19. Reaction of [Rh(η^5-C_5H_5)(PMe_3)(C_2H_4)] in pentafluoroanisole [42].

as shown in Fig. 19, reaction of this complex with 1 equiv. of $PPh_3C^+PF_6^-$ at 220 K generates [(η^5-C_5H_5)(PMe_3)Rh=CH(OC_6F_4)]PF_6.

Hughes et al. [43] have studied the reactions of the perfluoroisopropyl complex [RhI(η^4-$C_5H_5(CF(CF_3)_2)(PMe_3)_2$], with 1 equiv. of $TlBF_4$ or $TlPF_6$ yielding the new complex [RhI(η^5-$C_5H_4(CH(CF_3)_2)(PMe_3)_2$] in 90% yield. The tertiary C–F bond in the starting complex has been replaced by H, and the original η^4-cyclopentadiene has been converted to a η^5-cyclopentadienyl ligand. Investigation of the precipitate formed in the reaction, using X-ray microanalysis, indicates that it contains mostly Tl and F, with small amounts of I.

The source of H in the $CH(CF_3)_2$ group has been identified as the *endo*-H from the original cyclopentadiene ligand.

Hughes et al. [44] have described the synthesis and structures of two cationic complexes containing adjacent fluoroalkyl and water ligands, both of which undergo hydrolysis of a CF_2 group, the facility of which depends strongly on the hydrogen-bonding ability of the counterion. Addition of perfluorobenzyl complex [RhI(η^5-C_5Me_5)($CF_2C_6F_5$)(PMe_3)] or perfluoropropyl analogue [RhI(η^5-C_5Me_5)($CF_2CF_2CF_3$)(PMe_3)] to $AgBF_4$ in moist CH_2Cl_2 affords the cationic aqua complexes [Rh(η^5-C_5Me_5)($CF_2C_6F_5$)(H_2O)(PMe_3)]BF_4 and [Rh(η^5-C_5Me_5)($CF_2CF_2CF_3$)(H_2O)(PMe_3)]BF_4.

While perfluoropropyl complex [Rh(η^5-C_5Me_5)($CF_2CF_2CF_3$)(H_2O)(PMe_3)]BF_4 appears to be indefinitely stable on standing in solution at room temperature, perfluorobenzyl analogue [Rh(η^5-C_5Me_5)($CF_2C_6F_5$)(H_2O)(PMe_3)]BF_4 is cleanly transformed on standing overnight in $CDCl_3$ solution into pentafluorophenyl carbonyl complex [Rh(η^5-C_5Me_5)(C_6F_5)(CO)(PMe_3)]BF_4. HF can be observed in the volatiles, after vacuum transfer. A suggested mechanism is shown in Figs. 20 and 21; hydrolysis of the CF_2 group affords a coordinatively unsaturated pentafluorobenzoyl complex, which undergoes pentafluorophenyl migration into the vacant coordination site to afford [Rh(η^5-C_5Me_5)(C_6F_5)(CO)(PMe_3)]BF_4. The

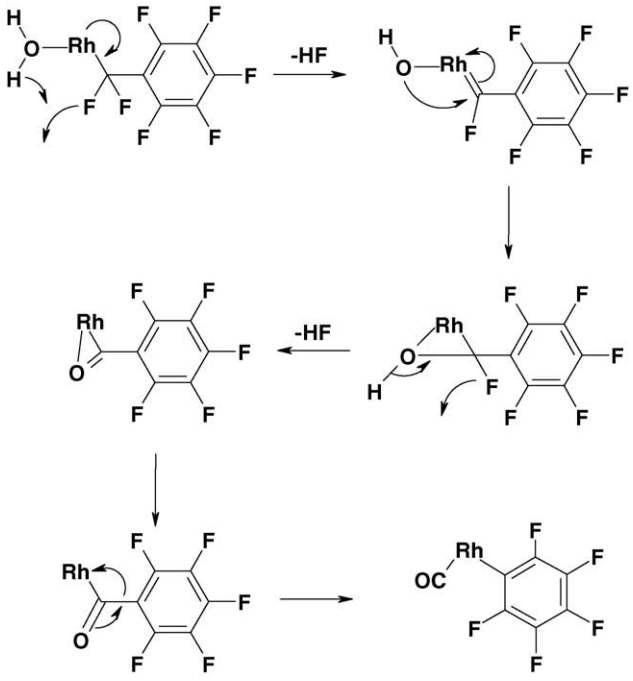

Fig. 20. Suggested mechanism for the formation of [Rh(η^5-C_5Me_5)(C_6F_5)(CO)(PMe_3)]BF_4 [44].

initial step is suggested to involve a proton from coordinated water acting as a fluoride acceptor with loss of fluoride enhanced by resonance stabilization from Rh; presumably the difference in reactivity of the CF_2 groups toward hydrolysis in perfluorobenzyl complex compared to perfluoropropyl analogue rests in additional enhancement of the leaving group ability of the benzylic fluoride.

The perfluoropropyl complex [RhI(η^5-C_5Me_5)($CF_2CF_2CF_3$)(PMe_3)] reacts with silver triflate to afford [Rh(SO_3CF_3)(η^5-C_5Me_5)($CF_2CF_2CF_3$)(PMe_3)] which treated with $NaBAr_4$ (Ar = 3,5-bis(trifluoromethyl)phenyl) in the presence of water results in rapid hydrolysis to give the perfluoroethyl carbonyl complex [Rh(η^5-

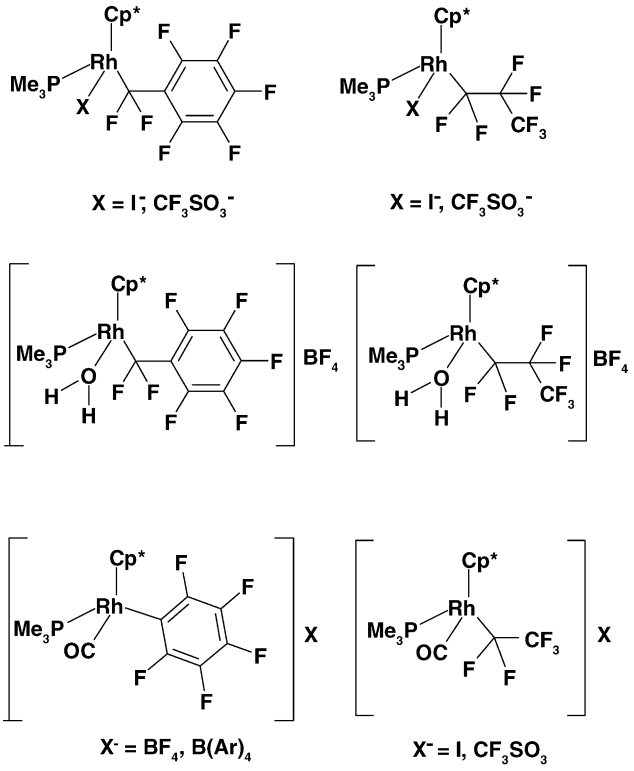

Fig. 21. Starting materials and products [44].

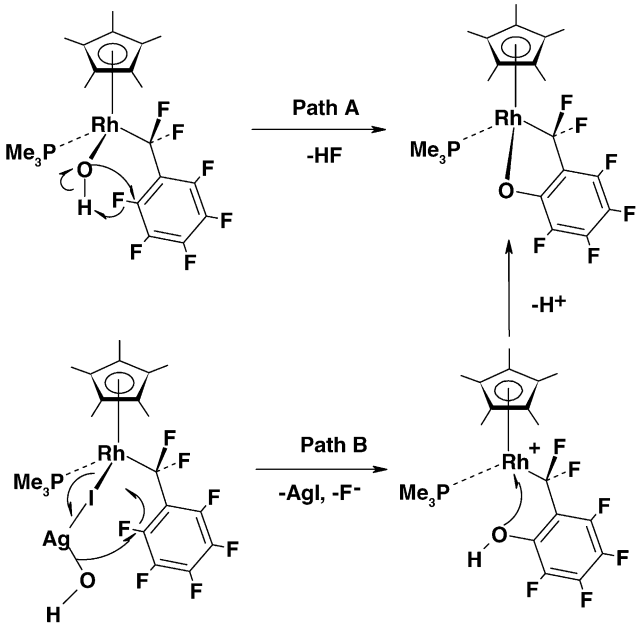

Fig. 22. Possible mechanism for the formation of [Rh(1,2-C_6F_4(O)(C=O))(η^5-C_5Me_5)(PMe_3)] [45].

C_5Me_5)(C_2F_5)(CO)(PMe_3)]BAr_4. The BF_4^- analogue was prepared unambiguously by the reaction of [Rh(η^5-C_5Me_5)(C_2F_5)I(PMe_3)] with $AgBF_4$ in the presence of CO. Each molecule exhibits close hydrogen-bonding interactions of coordinated water molecule with the tetrafluoroborate counterion.

Hughes et al. [45] have found that the perfluorobenzylrhodium complex [RhI(η^5-C_5Me_5)($CF_2C_6F_5$)(CO)], reacts with *N*-methylmorpholine-*N*-oxide (NMO) with loss of CO_2 and formation of the iodo-bridged dimer [Rh(μ^2-I)(η^5-C_5Me_5)($CF_2C_6F_5$)]$_2$. While attempts to prepare hydroxo complexes by reaction of [Rh(η^5-C_5Me_5)($CF_2C_6F_5$)(I)(PMe_3)], with sources of hydroxide were unsuccessful, treatment of [RhI(η^5-C_5Me_5)($CF_2C_6F_5$)(PMe_3)] with moist silver oxide affords the oxametallacycle [Rh(1,2-C_6F_4(O)(CF_2))(η^5-C_5Me_5)(PMe_3)], which undergoes rapid hydrolysis of the R–CF_2 group by adventitious moisture to afford the crystallographically characterized analogue [Rh(1,2-C_6F_4(O)(C=O))(η^5-C_5Me_5)(PMe_3)]. Two possible mechanisms are shown in Fig. 22.

Murai and co-workers [46] have discovered the first Rh-catalyzed, chelation-assisted Si–F exchange reaction between disilanes and fluoroarenes activated by ketone or oxazoline functionality *ortho* to the C–F bond (Fig. 23). The reaction of functionalized fluorobenzenes, such as fluoroacetophenones and (fluorophenyl)oxazolines, with $Me_3SiSiMe_3$ in the presence of a catalytic amount of a rhodium complex results in a site-selective Si–F exchange to give *ortho*-(trimethylsilyl)fluorobenzenes. The reaction involves cleavage of C–F bonds.

Young and Grushin [47] reported the first example of a transition metal-catalyzed hydrogenolysis of the C–F bond in monofluoroarenes, the most unreactive carbon–heteroatom single bond known (Fig. 24).

1-Fluoronaphthalene react with H_2 in toluene in the presence of 40% NaOH and catalytic amounts of [$RhCl_2$(H)(Cy_3P)$_2$] to give naphthalene (Fig. 24). Given the exceptionally poor reactivity of the substrate, the reaction occurs under mild conditions, i.e., 95 °C and 80 psi of H_2, furnishing naphthalene in >90% selectivity at 45% conversion (GC–MS) after 20 h. According to the authors, under rigorously oxygen-free conditions, hydrogenolysis is homogeneously catalyzed, as determined by the mercury test. Fluorobenzene, 4-fluorotoluene, 3-fluoroanisole and 4-fluoroaniline remained unreactive under similar O_2-free conditions. No reaction of C_6H_5F occurred in this system even in the presence of nucleophilic and/or Lewis acid promoters.

[Rh(dmgH)$_2$(PPh_3)]$^-$ ([Rh]$^-$), dmgH = (OHN=CHCH=NO)$^-$, synthesized by reduction of [Rh]–Cl with $NaBH_4$ in methanolic KOH, reacts with 1,ω-dihaloalkanes $X(CH_2)_nF$ (X = Cl, *n* = 1; X = Br, *n* = 3) forming [Rh]–CH_2F and [Rh]–$(CH_2)_3F$ [48]. Reaction of [Rh]$^-$ with $BrCH_2CH_2F$ affords instead of the expected 2-fluoroethyl complex the dinuclear complex [Rh]–CH_2CH_2–[Rh] exhibiting an unexpected C–F bond activation. It is suggested that the probable intermediate 2-fluoroethyl complex [Rh]–CH_2CH_2F reacts further to give the dimethylene-bridged dinuclear complex [Rh]CH_2CH_2[Rh] in an intermolecular substitution reaction.

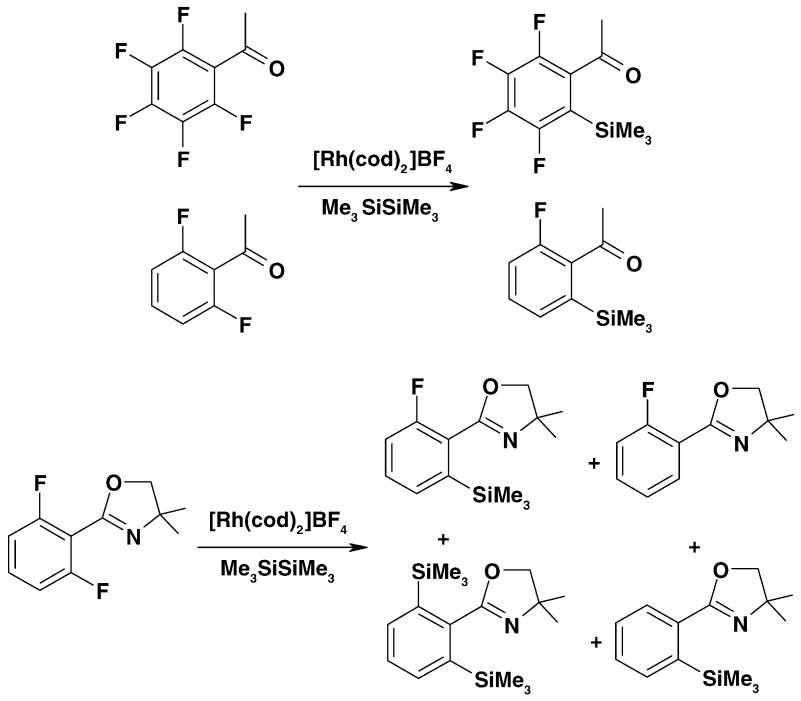

Fig. 23. Rh-catalyzed, chelation-assisted Si─F exchange reaction [46].

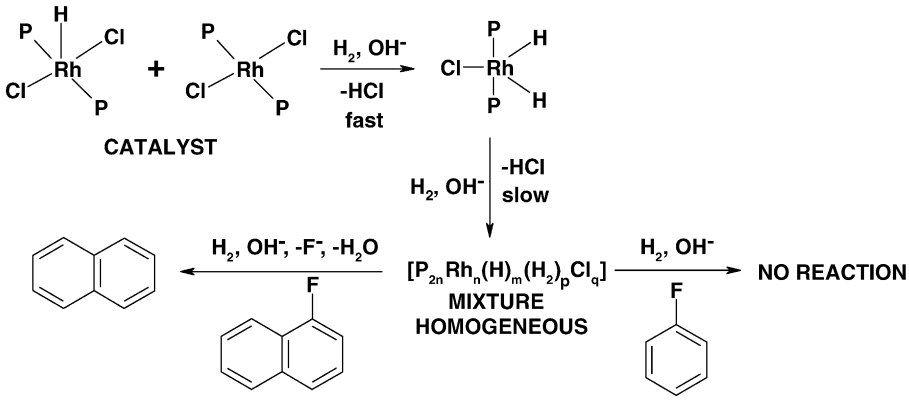

Fig. 24. Transition metal-catalyzed hydrogenolysis of the C─F bond in monofluoroarenes [47].

Braun and co-workers [49,50] have shown that reaction of $[RhH(PEt_3)_4]$ with hexafluoropropene affords the C–F activation product $[Rh((Z)\text{-}CF{=}CF(CF_3))(PEt_3)_3]$ as well as $Et_3P(F)((Z)\text{-}CF{=}CF(CF_3))$ as shown in Fig. 25.

In contrast, addition of (*E*)-1,2,3,3,3-pentafluoropropene to $[RhH(PEt_3)_4]$ yields $[Rh\{(E)\text{-}C(CF_3){=}CHF\}(PEt_3)_3]$ together with $[RhF(PEt_3)_3]$ and (*Z*)-1,3,3,3-tetrafuoropropene. As shown in Fig. 26, treatment of $[Rh\{(E)\text{-}C(CF_3){=}CHF\}(PEt_3)_3]$ with hydrogen effects the formation of 1,1,1-trifluoropropane and the fluoro compounds $[RhF(PEt_3)_3]$ and *cis-mer*-$[Rh(H)_2F(PEt_3)_3]$.

On treatment of $[RhF(PEt_3)_3]$ or of a mixture of $[RhF(PEt_3)_3]$ and *cis-mer*-$[Rh(H)_2F(PEt_3)_3]$ with $HSiPh_3$ the complexes $[RhH(PEt_3)_3]$ and *cis-fac*-$[Rh(H)_2(SiPh_3)(PEt_3)_3]$ are obtained. Both compounds are capable of the C–F activation of hexafluoropropene to afford $[Rh((Z)\text{-}CF{=}CF(CF_3))(PEt_3)_3]$. A possible mechanism of the C–F activation of fluorinated propene derivatives is depicted in Fig. 26.

A cyclic process for the hydrodefluorination of $CF_2{=}CFCF_3$ has been developed allowing the recovery of rhodium complexes, which are again suitable for C–F activation.

5. Iridium

Cundari and Vaddadi [51] have published a theoretical study considering the interactions of the fragment $[Ir(PH_3)_2(H)]$ with C–X species. In this research, the B3LYP density functional and Stevens effective core potentials are used to compare carbon–hydrogen and carbon–heteroatom

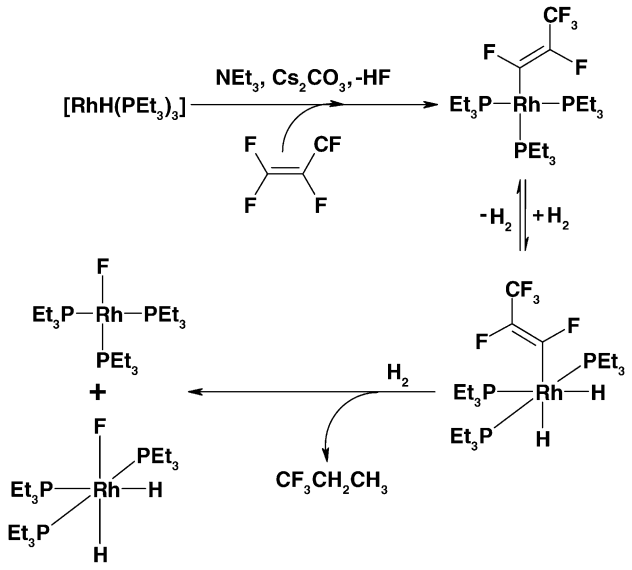

Fig. 25. Reaction of $[RhH(PEt_3)_4]$ with hexafluoropropene [50].

bond activation by an iridium(I) complex. Of particular importance is to address the kinetic (transition state) and thermodynamic (ground state) selectivity. The complex $[Ir(H)(PH_3)_2]$ with CH_3–X (X = F, Cl, OH, SH, NH_2, PH_2) as the substrate has been used as a model. Good agreement in geometries is obtained between the target molecules and experimental models. The resultant products of C–H and C–X oxidative addition are Y-shaped minima (i.e., a distorted trigonal bipyramid with one acute and two obtuse angles among the equatorial ligands). Oxidative addition of the C–X bond to the substrate is exothermic for groups 16 and 17, but endothermic for group 15. A significant thermodynamic preference for C–X activation over C–H activation is observed for these Ir(I) complexes. However, analysis of the transition states for oxidative addition suggests that there is a kinetic preference for C–H activation.

Su and Chu [31] reported in 1997 one of the first theoretical studies of C–F activation. They showed that oxidative addition of the C–F bond of CH_3–F to 3-coordinated 14-electron $[M(X)(PH_3)_2]$ (M = Rh, Ir; X = CH_3, H, Cl) is thermodynamically favorable. The reaction was most favorable and had the smallest activation barrier for $[Ir(Cl)(PH_3)_2]$. This work is summarized in Section 4.

Roper and co-workers [52] studied the reaction of the tetrafluoroethylene complex $[IrCl(\eta^2\text{-}C_2F_4)(PPh_3)_2]$ with HCl or Cl_2 to obtain $[IrCl_2(CF_2CF_2H)(PPh_3)_2]$ or $[IrCl_2(CF_2CF_2Cl)(PPh_3)_2]$, respectively. These coordinately unsaturated complexes react with various neutral ligands to give stable, six-coordinated, tetrafluoroethyl and halotetrafluoroethyl complexes. As shown in Fig. 27, the acetonitrile derivative $[IrCl_2(CF_2CF_2H)(CH_3CN)(PPh_3)_2]$ undergoes a reaction with HCl that proceeds through the intermediate fluorocarbene complex, $[IrCl_2(=CFCF_2H)(CH_3CN)(PPh_3)_2]^+$, to give, upon hydrolysis, $[IrCl_2(C(O)CF_2H)(CH_3CN)(PPh_3)_2]$. Thermal treatment of any of the acyl complexes results finally, as shown in Fig. 28, in a reverse migration process and formation of $[IrCl_2(CF_2H)(CO)(PPh_3)_2]$.

Perera et al. [53] have shown that when *Z,E*-$PPh_2CH_2C(Bu^t)$=N–N=$CH(C_6F_5)$ was heated in benzene with $[IrCl(CO)_2$(*p*-toluidine)] it gave the cyclometallated dichlorocarbonyliridium(III) complex $[IrCl_2(CO)$

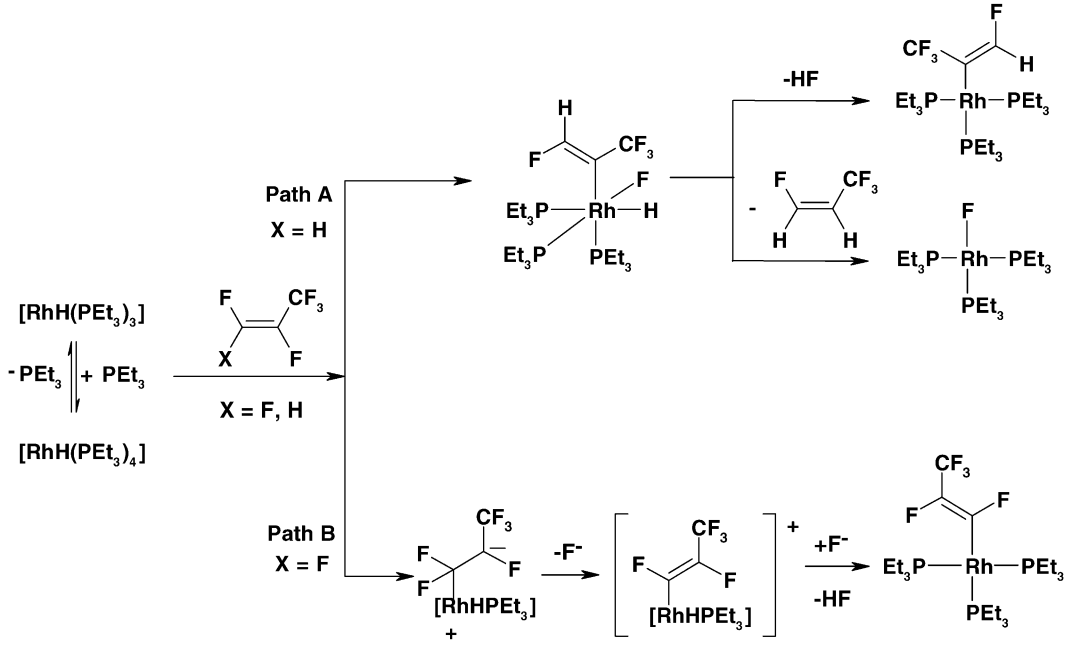

Fig. 26. A possible mechanism of the C–F activation of fluorinated propene derivatives [50].

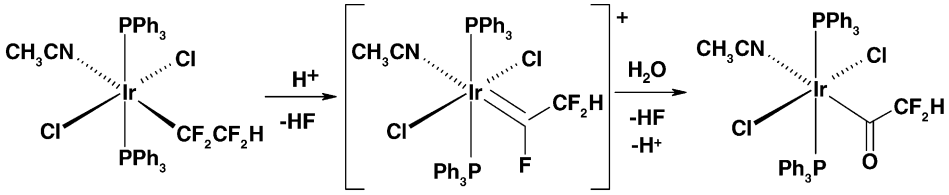

Fig. 27. Formation of $[IrCl_2(C(O)CF_2H)(CH_3CN)(PPh_3)_2]$ [52].

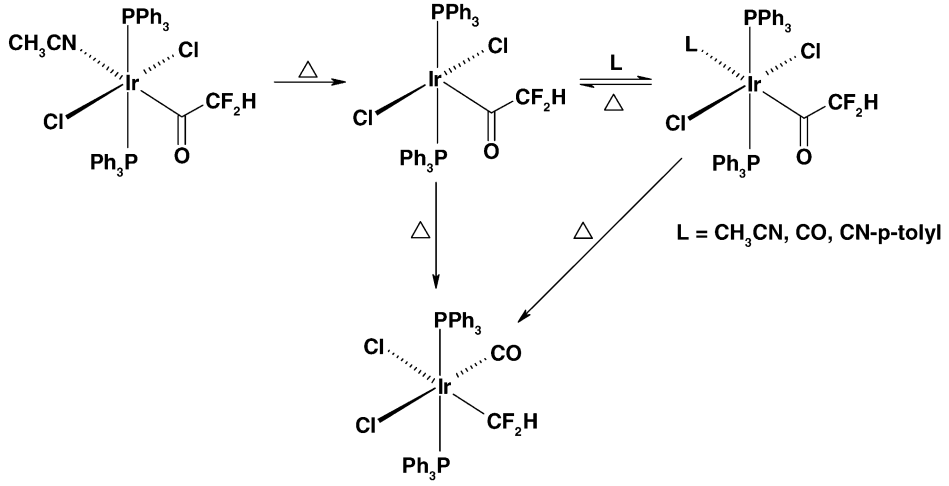

Fig. 28. Formation of $[IrCl_2(CF_2H)(CO)(PPh_3)_2]$ [52].

$(PPh_2CH_2C(Bu^t)=N–N=CH(C_6F_4))]$ (Fig. 29) the formation of which involved a C–F bond fission.

Hughes et al. [54,55] have made invaluable contributions to understand the chemistry involved in the process of carbon–fluorine bond activation using different variations of the fragment $[Ir(\eta^5\text{-}C_5R_5)L_n]$.

They reported the first examples of hydrogenolysis of the α-CF_2 groups in some iridium fluoroalkyls using dihydrogen under ambient conditions. Treating methylene chloride solutions of the cationic (aqua)(fluoroalkyl)iridium complexes $[Ir(\eta^5\text{-}C_5Me_5)(CF_2Rf)(H_2O)(PMe_3)]BF_4$ (Rf = CF_3 or CF_2CF_3) with dihydrogen results in clean and rapid formation of the known iridium trihydride $[Ir(\eta^5\text{-}C_5Me_5)(H)_3]BF_4$. The fate of the fluoroalkyl ligand was an approximately 1:1 mixture of two hydrofluorocarbon (HFC) compounds, identified as $RfCFH_2$ and $RfCH_3$ (Rf = CF_3, CF_3CF_2) by ^{19}F NMR spectroscopy. No trace of the monohydrogenated species CF_3CF_2H or $CF_3CF_2CF_2H$ were observed. Similarly, treatment of the corresponding perfluoroisopropyl complex $[Ir(\eta^5\text{-}C_5Me_5)(CF(CF_3)_2)(H_2O)(PMe_3)]BF_4$ with H_2 affords only $[Ir(\eta^5\text{-}C_5Me_5)(H)_3]BF_4$ and $CF_3CH_2CF_3$ with no observable trace of CF_3CFHCF_3 (Fig. 30). These observations represent the first examples of the hydrogenolysis of aliphatic C–F bonds in the coordination sphere of a transition metal. Furthermore, the reaction is selective for H_2, with no observable hydrolysis of the fluoroalkyl group, even in the presence of the water originally present in the coordination sphere.

Reaction of $[Ir(\eta^5\text{-}C_5Me_5)(PMe_3)(CF_2CF_3)H]$ with CH_3CO_2D affords mostly $[Ir(\eta^5\text{-}C_5Me_5)(PMe_3)(CFHCF_3)(O_2CCH_3)]$, while the corresponding reaction of $[Ir(\eta^5\text{-}C_5Me_5)(PMe_3)(CF_2CF_3)D]$ with CH_3CO_2H affords mostly $[IrCp^*(PMe_3)(CFDCF_3)(O_2CCH_3)]$. These results are consistent with external protonation of the C–F bond and

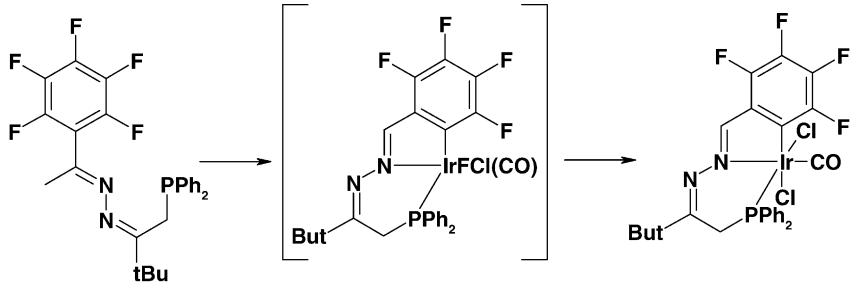

Fig. 29. Formation of $[IrCl_2(CO)(PPh_2CH_2C(Bu^t)=N–N=CH(C_6F_4))]$ [53].

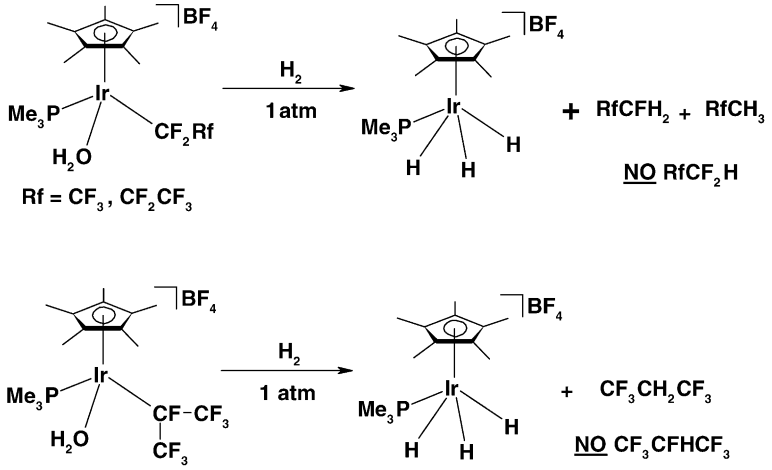

Fig. 30. Reactions of $[Ir(\eta^5\text{-}C_5Me_5)(Rf)(H_2O)(PMe_3)]BF_4$ [54].

migration of the originally present H (or D) from Ir to C and suggest that the previously reported CF bond hydrogenolysis using dihydrogen proceeds via heterolytic activation of the H_2 molecule at iridium.

As a result of these experiments, the role of the metal in the reaction of $[Ir(\eta^5\text{-}C_5Me_5)(CF_2Rf)(H_2O)(PMe_3)]BF_4$ with H_2, is defined as shown in Fig. 31. Binding of H_2 to the cationic iridium center of $[Ir(\eta^5\text{-}C_5Me_5)(CF_2CF_3)(H_2O)(PMe_3)]BF_4$ results in displacement of water and heterolytic activation of H_2 to give $[IrH(\eta^5\text{-}C_5Me_5)(=CFCF_3)(PMe_3)]$, C–F activation occurs by protonation of the α-CF bond by external acid to produce HF, and migration of the hydride ligand to carbon generates the new CH bond. In the absence of a good coordinating anion, more H_2 binds to repeat the process. Now there is an apparent competition between protonation at the Ir–C bond to afford elimination of CF_3CFH_2 or protonation at the remaining C–F bond to repeat the C–F activation process, leading eventually to elimination of CF_3CH_3. A similar proton-promoted C–F activation in a cationic iridium complex containing a CF_3 ligand has been shown to be triggered by heterolytic activation of H_2, but hydrolysis to a CO ligand by adventitious moisture is the outcome, rather than the alternatively available H migration.

The HFC products themselves are of unusual interest; CF_3CFH_2 (HFC-134a) is the replacement refrigerant for CF_2Cl_2 (CFC-12), and similar HFCs are used as inhalation anesthetics.

Hughes et al. [56] have found that reactions of $[IrI(Rf)(\eta^5\text{-}C_5Me_5)(PMe_3)]$ (Rf = $CF_2CF_2CF_3$, $CF(CF_3)_2$) with either $NaBH_4$ or $LiAlH_4$ afford i.a. iridium hydrides $[IrH(C_5Me_5)(CH{=}CFCF_3)(PMe_3)]$ or $[IrH(C_5Me_5)(C(CF_3){=}CF_2)(PMe_3)]$, in which the fluoroalkyl groups are converted to unsaturated ligands via apparent α-CF activation and elimination of HF (Fig. 32). A clean and selective route to desired saturated fluoroalkyl-(hydrido) complexes $[IrH(C_5Me_5)(Rf)(PMe_3)]$ (Rf = $CF_2CF_2CF_3$, CF_2CF_3, $CF(CF_3)_2$) is afforded by treatment of the aqua cations $[Ir(C_5Me_5)(Rf)(H_2O)(PMe_3)]BF_4$ with 1,8-bis(dimethylamino)-naphthalene, "Proton Sponge".

Hughes et al. [57,58] have prepared the first transition metal complex of tetrafluorobenzyne, $[Ir(\eta^5\text{-}C_5Me_5)(PMe_3)(\eta^2\text{-}C_6F_4)]$. The experimental approach is shown in Fig. 33. Pentafluorophenyl complex $[IrI(\eta^5\text{-}$

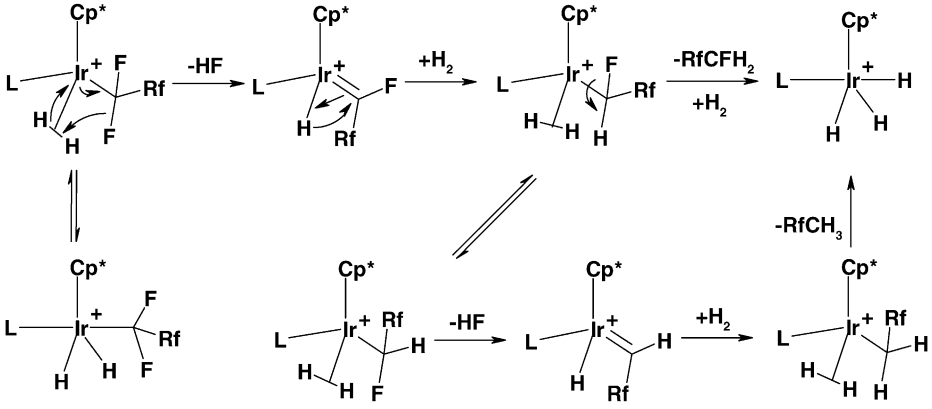

Fig. 31. Stepwise reactions of $[Ir(\eta^5\text{-}C_5Me_5)(CF_2Rf)(H)_2L]$ [54].

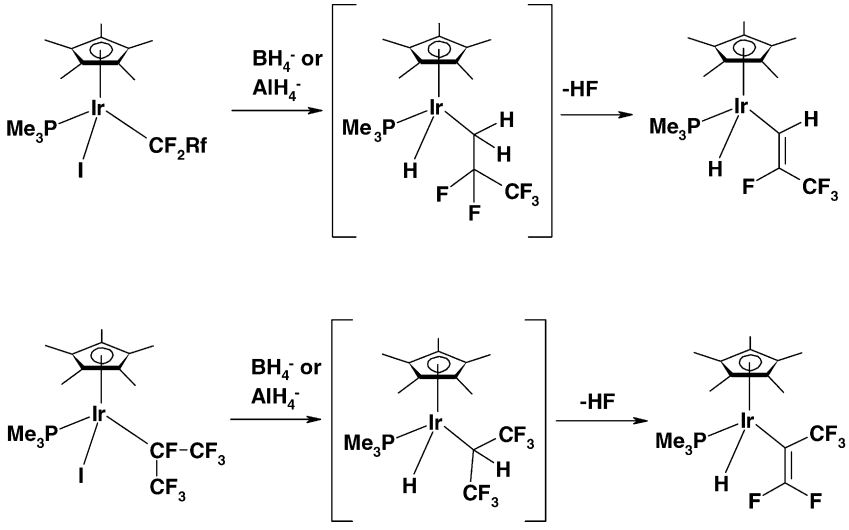

Fig. 32. Reactions of $[IrI(\eta^5\text{-}C_5Me_5)(Rf)(PMe_3)]$ [56].

$C_5Me_5)(C_6F_5)(CO)]$ is prepared by oxidative addition of iodopentafluorobenzene to $[Ir(\eta^5\text{-}C_5Me_5)(CO)_2]$. This reaction requires prolonged refluxing in benzene, while the corresponding perfluoroalkyl iodides react at room temperature. Choice of solvent is also important; no reaction is observed in refluxing hexane, and refluxing toluene affords products that do not contain C_6F_5 ligands. Carbonyl displacement with PMe_3 affords $[Ir(\eta^5\text{-}C_5Me_5)I(C_6F_5)(PMe_3)]$, which can be converted to the corresponding aqua cation $[Ir(\eta^5\text{-}C_5Me_5)(C_6F_5)(H_2O)(PMe_3)]^+$ using AgOTf in moist toluene. As observed with analogous perfluoroalkyl(aqua) complexes, treatment of $[Ir(\eta^5\text{-}C_5Me_5)(C_6F_5)(H_2O)(PMe_3)]^+$ with 1,8-bis(dimethylamino)-naphthalene (Proton Sponge) cleanly affords the hydride $[Ir(\eta^5\text{-}C_5Me_5)(C_6F_5)(H)(PMe_3)]^+$. This hydride is obtained less cleanly by direct reaction of $[Ir(\eta^5\text{-}C_5Me_5)I(C_6F_5)(PMe_3)]$ with $NaBH_4$, and has also been prepared recently by Bergman and co-workers by reaction of the nucleophilic anion $[Ir(\eta^5\text{-}C_5Me_5)(PMe_3)H]^-Li^+$ with hexafluorobenzene [59]. Finally, treatment of the hydride $[Ir(\eta^5\text{-}C_5Me_5)(C_6F_5)(H)(PMe_3)]^+$ with an excess of *n*-BuLi affords the benzyne complex $[Ir(\eta^5\text{-}C_5Me_5)(PMe_3)(\eta^2\text{-}C_6F_4)]$, presumably via deprotonation to give the intermediate shown in Fig. 33, followed by elimination of LiF.

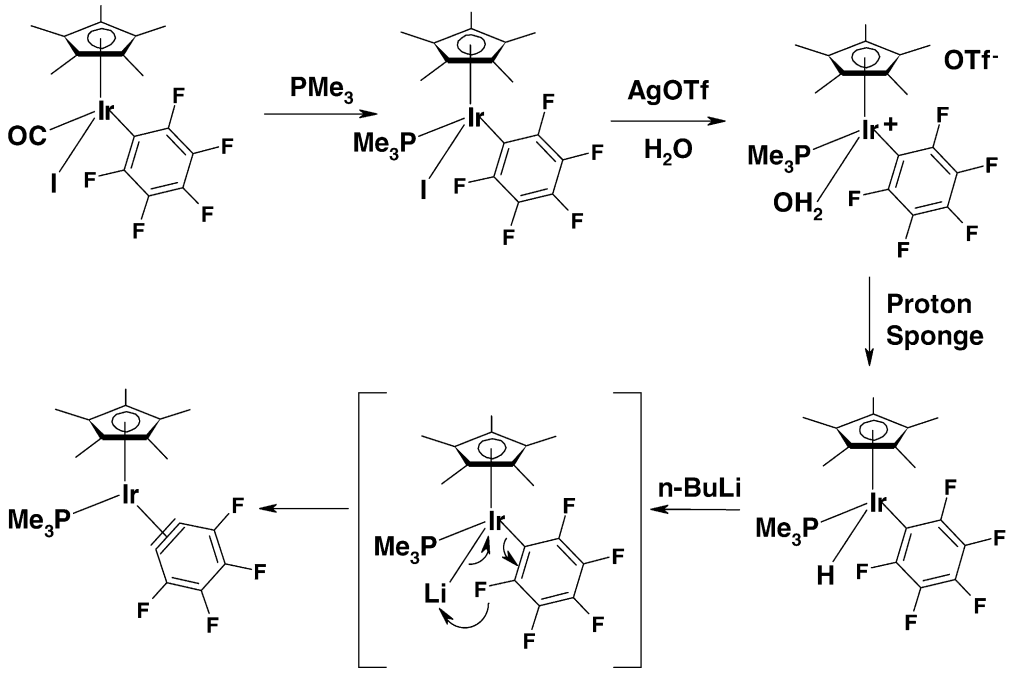

Fig. 33. Synthesis of $[Ir(\eta^5\text{-}C_5Me_5)(PMe_3)(\eta^2\text{-}C_6F_4)]$ [57].

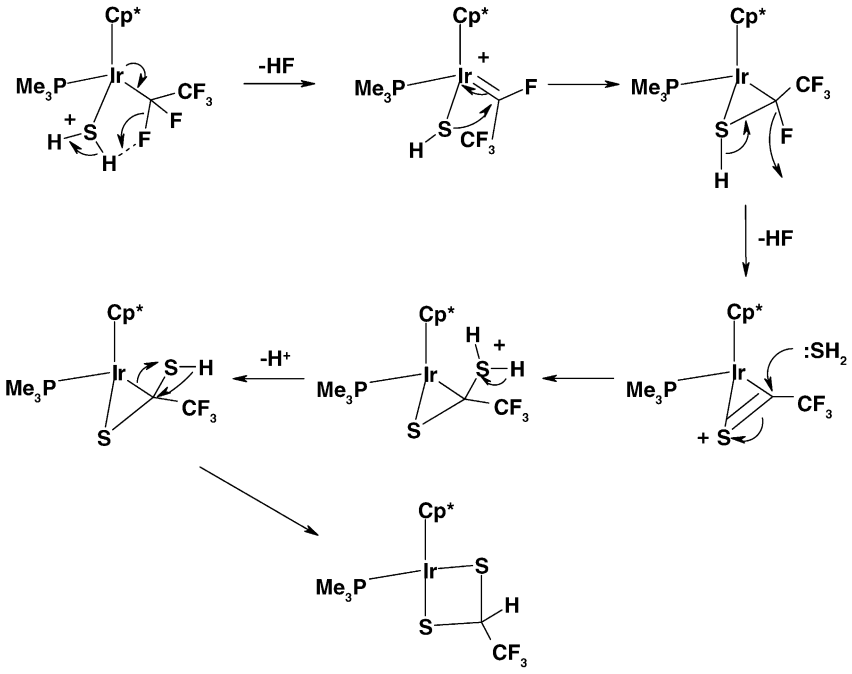

Fig. 34. Stepwise mechanism yielding [Ir(η^5-C_5Me_5)(PMe_3)(*syn*-S_2CHCF_3)] [60].

Treatment of the tetrafluorobenzyne complex [Ir(η^5-C_5Me_5)(η^2-C_6F_4)(PMe_3)] with $MeCO_2H$ affords the tetrafluorophenyl complex [Ir(η^5-C_5Me_5)(2,3,4,5,-C_6F_4H)(PMe_3)(O_2CMe)], which, on treatment with $NaBH_4$, affords the hydride complex [IrH(η^5-C_5Me_5)(2,3,4,5-C_6F_4H)(PMe_3)] which treated with *n*-BuLi affords the trifluorobenzyne complex [Ir(η^5-C_5Me_5)(3,4,5-C_6F_3H)(PMe_3)]. Treatment of [Ir(η^5-C_5Me_5)(3,4,5-C_6F_3H)(PMe_3)] with $MeCO_2H$ gives a mixture of two protonation products, [Ir(η^5-C_5Me_5)(2,3,4-$C_6F_3H_2$)(PMe_3)(O_2CMe)] and [Ir(η^5-C_5Me_5)(3,4,5-$C_6F_3H_2$)(PMe_3)(O_2CMe)] in an 8:1 ratio.

Dimethyl sulfide [60] reacts with [Ir(η^5-C_5Me_5)(Rf)(PMe_3)(H_2O)]BF_4 (Rf = $CF(CF_3)_2$, CF_2CF_3) to afford [Ir(Rf)(η^5-C_5Me_5)(PMe_3)(Me_2S)]BF_4. In contrast (Fig. 34), H_2S reacts with the secondary fluoroalkyl complex [Ir(η^5-C_5Me_5)(PMe_3)($CF(CF_3)_2$)(H_2O)][BF_4] to give the sulfhydryl complex [Ir(η^5-C_5Me_5)(PMe_3)($CF(CF_3)_2$)(SH)] and with [Ir(η^5-C_5Me_5)(PMe_3)(CF_2CF_3)(H_2O)]BF_4 to give carbon–fluorine bond activation with formation of a mixture of compounds containing two new classes of fluorinated ligands. The molecular structures of representatives of each class, the 2,3-dithiametallacyclobutane complex [Ir(η^5-C_5Me_5)(PMe_3)(*syn*-S_2CHCF_3)] and the 2,4,6-trithiametallacyclohexane complex [Ir(η^5-C_5Me)(PMe_3)(*anti*,*anti*-$S_3\{CHCF_3\}_2$)], have been determined. Both *syn* and *anti* stereoisomers of the dithiametallacyclobutane complex and all three stereoisomers (*syn–syn*, *syn–anti* and *anti–anti*) of the trithiametallacyclohexane complex are observed in solution as products of the reaction, and their configurations have been confirmed by NOE experiments.

Hughes et al. [61] have shown that reaction of iridium–fluoroalkyl complexes with fluoride acceptors occurs with completely diastereoselective activation of a C–F bond and formation of a new C–C bond. Protonation occurs with complete selectivity at the C–F bond without any detectable formation of methane by protonation at the Ir–CH_3 group. [Ir(η^5-C_5Me_5)(CH_3)($CF_2CF_2CF_3$)(PMe_3)] reacts with HCl (2,6-lutidinium chloride) as shown in Fig. 35, to give a single diastereomer of [Ir(η^5-C_5Me_5)Cl($CF(CH_3)(CF_2CF_3)$)(PMe_3)]. A similar reaction with $CF_3CO_2^-$ yields the compound [Ir(η^5-C_5Me_5)(CF_3CO_2)($CF_2CFHCF_2CF_3$)(PMe_3)] (Fig. 35). The proposed sequence of reactions in this interesting process includes i.a. both H and CH_3 migration, β-hydrogen elimination and alkene rotation.

Hughes et al. [62] have also discovered an unexpected route to the only known tetrafluorobutatriene transition metal complex [Ir(η^5-C_5Me_5)(2,3-η^2-CF_2=C=C=CF_2)(PMe_3)]. To this end, the starting complexes [Ir(η^5-C_5Me_5)(I)($CF(CF_3)_2$)(PMe_3)] and [Ir(η^5-C_5Me_5)(I)($CF(CF_2CF_3)(CF_3)_2$)(PMe_3)] were prepared by oxidative addition of the appropriate secondary perfluoroalkyl iodide to [Ir(η^5-C_5Me_5)($CO)_2$], followed by carbonyl displacement by PMe_3. Treatment of [Ir(η^5-C_5Me_5)(I)($CF(CF_3)_2$)(PMe_3)] with 3 equiv. of sodium naphthalenide ($NaC_{10}H_8$) in THF afforded the previously reported unsaturated hydride complex [Ir(η^5-C_5Me_5)(H)($C(CF_3)$=CF_2)(PMe_3)] with apparent reductive loss of iodide and two fluoride anions. The source of the hydride is presumably the reaction solvent. Two equivalents of $NaC_{10}H_8$ affords a mixture of [Ir(η^5-C_5Me_5)(H)($C(CF_3)$=CF_2)(PMe_3)] and the corresponding

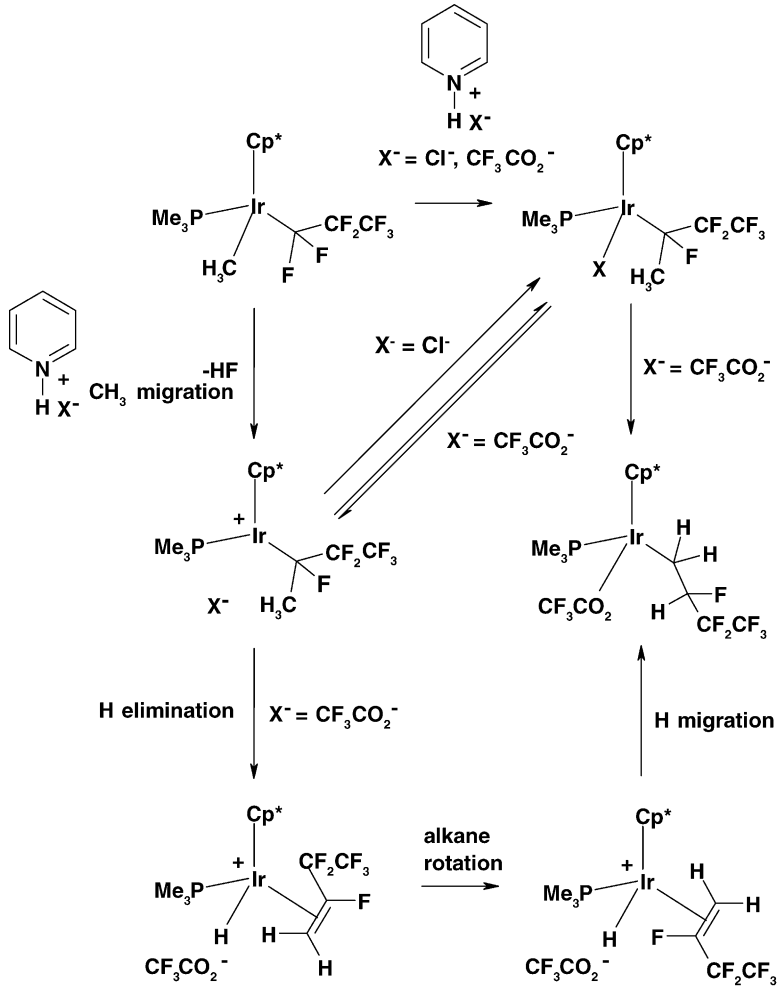

Fig. 35. Proposed sequence of reactions [61].

iodo analogue [Ir(η^5-C_5Me_5)(I)(C(CF_3)=CF_2)(PMe_3)] and more than 3 equiv. of $NaC_{10}H_8$ results in no further reaction of [Ir(η^5-C_5Me_5)(H)(C(CF_3)=CF_2)(PMe_3)]. In contrast, the *sec*-butyl analogue reacts with 6 equiv. of $NaC_{10}H_8$ to afford the tetrafluorobutatriene complex [Ir(η^5-C_5Me_5)(η^2-CF_2=C–C=CF_2)(PMe_3)]. Fewer than 6 equiv. of $NaC_{10}H_8$ affords a complex mixture of products, some of which clearly contain Ir–H bonds by NMR spectroscopy.

The fluorovinyl [63] complexes [Ir_2(CF=CF_2)(CH_3)($CO)_2$(μ-Cl)(dppm)$_2$]CF_3SO_3 and [Ir_2(C(H)=CF_2)(CH_3)($CO)_2$(μ-Br)(dppm)$_2$]CF_3SO_3 are prepared by the oxidative addition of ClFC=CF_2 and BrHC=CF_2, respectively, to [Ir_2(CH_3)($CO)_2$(dppm)$_2$]CF_3SO_3. Both compounds have the methyl and fluorovinyl groups on different metals essentially opposite to the metal–metal bond. Protonation of [Ir_2(CF=CF_2)(CH_3)($CO)_2$(μ-Cl)(dppm)$_2$]CF_3SO_3 occurs at the Ir–Ir bond to give [Ir_2(CF=CF_2)(CH_3)($CO)_2$(μ-Cl)(μ-H)(dppm)$_2$]($CF_3SO_3)_2$. Attempts to remove the chloride ligand from [Ir_2(CF=CF_2)(CH_3)($CO)_2$(μ-Cl)(dppm)$_2$]CF_3SO_3 or to replace it with hydride or methyl groups failed. Instead, the reaction of [Ir_2(CF=CF_2)(CH_3)($CO)_2$(μ-Cl)(dppm)$_2$]CF_3SO_3 with methyllithium resulted in replacement of one fluoride substituent on the trifluorovinyl group by a methyl group to give [Ir_2(CF=CFCH_3)(CH_3)($CO)_2$(μ-Cl)(dppm)$_2$]CF_3SO_3 (see Fig. 36). The X-ray structural determination of this compound indicates that replacement of a fluoride *trans* to the Ir–C_2F_3 bond has occurred and that migration of the resulting methyldifluorovinyl group to the metal bearing the methyl ligand has occurred. Therefore the fluorine atom *trans* to Ir in the trifluorovinyl complex [Ir_2(CF=CF_2)(CH_3)($CO)_2$(μ-Cl)(dppm)$_2$]CF_3SO_3 can be selectively replaced by a methyl group, and the authors propose that this occurs via a fluoroalkylidene-bridged intermediate.

Eisenberg and co-workers [64] have shown that the cationic iridium(III) complex [IrCF_3(CO)(dppe)(*o*-$C_6H_4I_2$)](B(3,5-(C_6H_3($CF_3)_2)_4)_2$ (dppe = 1,2-bis(diphenylphosphino)ethane) undergoes reaction in the presence of dihydrogen to form [IrH_2($CO)_2$(dppe)] as the major product. Through labeling studies and ^{1}H and ^{31}P-{^{1}H} NMR spectroscopies including parahydrogen measurements, it is shown

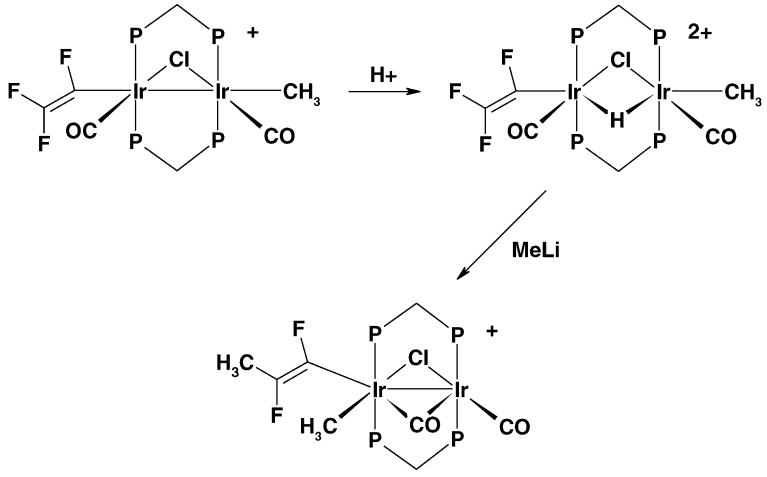

Fig. 36. Formation of $[Ir_2(CF{=}CFCH_3)(CH_3)(CO)(\mu\text{-}CO)(\mu\text{-}Cl)(\mu\text{-}dppm)_2]CF_3SO_3$ [63].

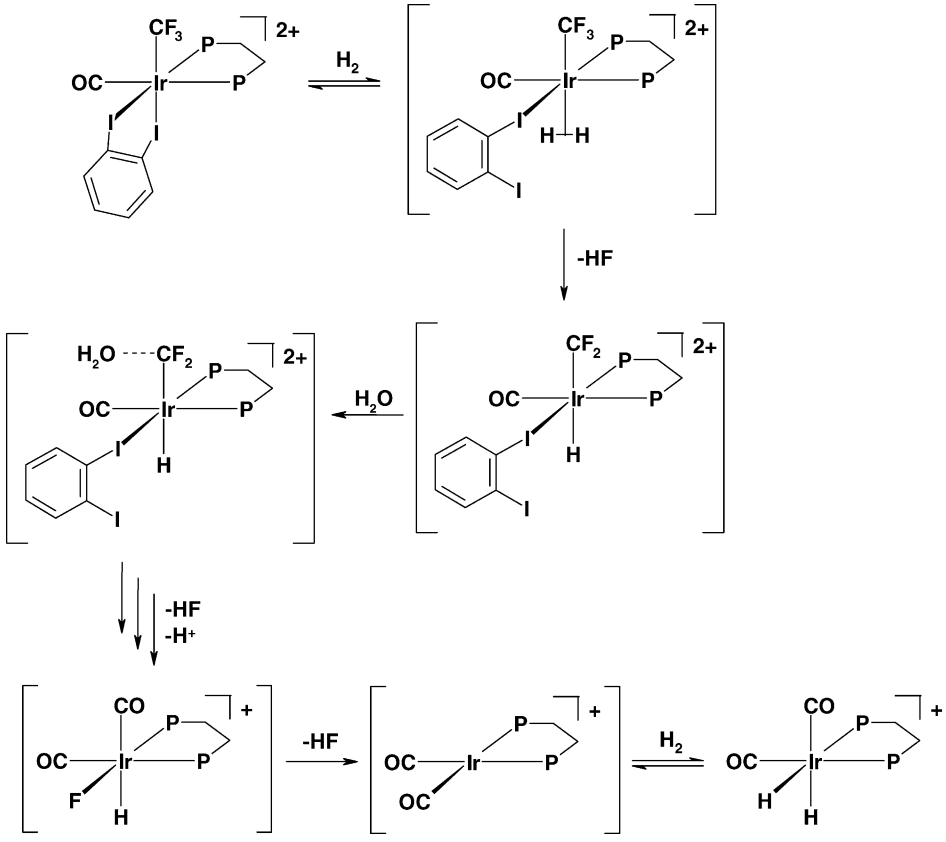

Fig. 37. Reaction sequence yielding $[IrH_2(CO)_2(dppe)]$ [64].

that the reaction involves conversion of the coordinated CF_3 ligand into carbonyl. In this reaction sequence (Fig. 37), the initial step is the heterolytic activation of dihydrogen, leading to proton generation which promotes α-C–F bond cleavage. Polarization occurs in the final $[IrH_2(CO)_2(dppe)]$ product by the reaction of H_2 with the Ir(I) species $[Ir(CO)_2(dppe)]$ that is generated in the course of the CF_3 to CO conversion.

6. Palladium

Smurnyi et al. [65] have studied the oxidative addition of methane and fluoromethane to nickel, palladium and platinum atoms and to their diphosphine and ethylenediphosphine complexes using a unique approach by the density functional theory with the PBE functional and the TZ2p basis set

taking into account relativistic corrections (the SBK effective core potential). The complete reaction paths were determined, and the saddle points were identified by calculating the Hessians. The reactions under consideration (except the dissociation of the C–H bond with the participation of atomic platinum, which was a barrierless reaction) involved the stage of formation of donor–acceptor prereaction complexes. The electrophilic and nucleophilic reaction phases were discovered. The barriers to reactions were found to decrease, and the heats of reactions to increase along the series of metals Pd, Ni, Pt, and along the series of complexes $M(PH_3)_2$, $M(PH_2CH_2CH_2PH_2)$. Fluoromethane was more active than methane. The conclusion was drawn that the oxidative addition of fluoromethane at the C–H bond was a kinetically controlled reaction, and the addition at the C–F bond was more favorable under thermodynamically controlled conditions.

Kambe and co-workers [66] have studied cross-coupling reactions of alkyl derivatives with Grignard reagents and disclosed the first example of a catalytic C–C bond-forming reaction using nonactivated alkyl fluorides (Eq. (4)):

$$^{n}C_8H_{17}{-}F + {}^{n}C_3H_7{-}MgBr \xrightarrow[\text{1,3-butadiene}]{PdCl_2} {}^{n}C_{11}H_{24} \quad (4)$$

For example, a reaction using 2 mmol of $^{n}C_8H_{17}$–F, 3 mol% catalyst, 1,3-butadiene (mol% based on the substrate), and $^{n}C_3H_7$–MgBr (2 equiv., 1 M), in THF, 25 °C and 3 h, $PdCl_2$ yields 23% $^{n}C_{11}H_{24}$, 1% $^{n}C_8H_{18}$ and 4% of a mixture of 1-octene and 2-octene.

Rzepa and co-workers [67] have published an ab initio molecular orbital study using both gas-phase and B3LYP/DZVP-COSMO solvation models of the mechanism of palladium insertion into alkyne and aryl carbon–halogen bonds. Their results suggest that the mechanism of palladium insertion into alkyne species can proceed via a concerted oxidative addition across the carbon–halogen bond. A stepwise mechanism via a σ-complex is favored when a nitro group is introduced onto the alkyne. The palladium insertion into variously substituted aryl fluorides was again found to proceed via a single-step concerted mechanism, and although a σ-complex can be located when 2,4-dinitro and 2-nitro substitution is present, the energy of this stepwise route is very similar to the concerted pathway and no clear decision on the pathway can be made. No intermediate σ-complex could be located for η^6-tricarbonylchromium-complexed fluorobenzene, and only a concerted pathway was identified.

Widdowson and Wilhelm [68,69] have found that (fluoroarene)-tricarbonylchromium(0) complexes undergo Suzuki and Stille cross-coupling reactions to form functionalized biaryl and styrene complexes in the presence of a palladium catalyst.

Several experiments with the Susuki system provide strong evidence for direct participation of the fluorobenzene complex in the coupling process with the implication of an unprecedented oxidative addition of the C–F bond to the palladium(0) intermediate. Whether this is a concerted insertion (Fig. 38, path A) or an addition–elimination sequence (Fig. 38, path B) via an *exo*addition of palladium to form **1** followed by fluoride loss to produce **2** cannot be determined at this point. The insertion product could be active in the catalytic cycle in either neutral (**3**) or cationic (**2**) form.

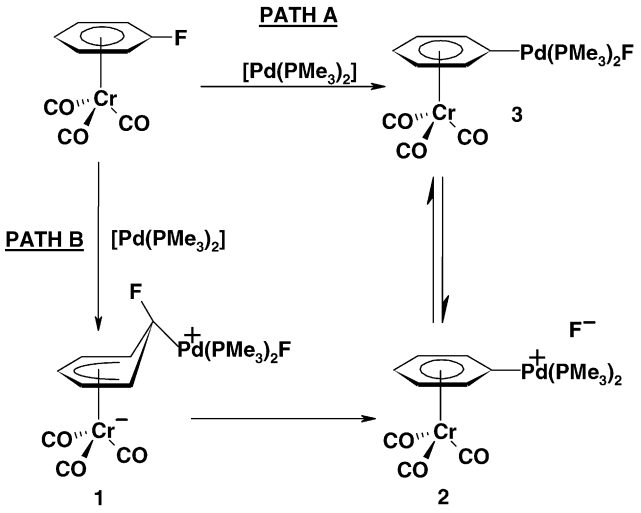

Fig. 38. Oxidative addition of the C—F bond to the palladium(0) intermediate [68].

The Suzuki reactions were optimal with [Pd_2(dibenzylideneacetone)$_3$]–PMe_3–Cs_2CO_3 in $MeOCH_2CH_2OMe$ at reflux. The Stille reactions were optimal with [Pd_2(dibenzylideneacetone)$_3$]–PMe_3–CsF in $MeOCH_2CH_2OMe$ at reflux and neither was adversely affected by a methoxy group on the complexed ring. The Suzuki reaction tolerated methyl, methoxy and a chloro group on the arylboronic acid ring but not a bromo group.

Widdowson and Wilhelm [70] have also reported the first successful palladium-catalyzed Suzuki reaction of an uncomplexed fluoroarene (Fig. 39).

4-Chlorobenzeneboronic acid gave the coupled product in 66% yield, which showed, remarkably, that the C–Cl bond of the chlorobenzeneboronic acid was less reactive in cross-coupling than the C–F bond of the fluoroarene under these conditions. An even more intriguing result was found with the coupling of 3-aminobenzeneboronic acid hemisulfate which gave the coupled product in 50% yield. Clearly, the amino-function, whether protonated or not, is insufficiently nucleophilic to compete with the palladium(0) species for the 2,4-dinitrofluorobenzene reagent.

Mi Kim and Yu [71] have studied the palladium(0)-catalyzed amination, Stille coupling and Suzuki coupling reactions of electron-deficient aryl monofluorides.

A set of control experiments were designed and performed to rule out (i) thermal reactions (neither Pd nor the ligand was present), (ii) influence of the ligand alone (no Pd was present), (iii) influence of the Pd(0) source alone (no ligand was present) and (iv) influence of Pd(II) species.

Pd(0) in the form of [Pd_2(dibenzylideneacetone)$_3$] did promote the amination, although far less effectively than

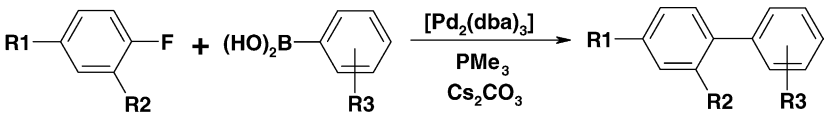

R1 = NO_2, H, CF_3, Me, MeO
R2 = NO_2
R3 = H, 2-MeS, 4-MeO, 2-MeO, 4-Cl, 3-NH_2, 4-^{t}Bu,

Fig. 39. Suzuki reactions of uncomplexed fluoroarenes [70].

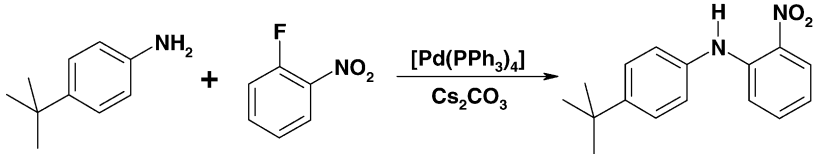

Fig. 40. Amination reaction with $[Pd(PPh_3)_4]$ [71].

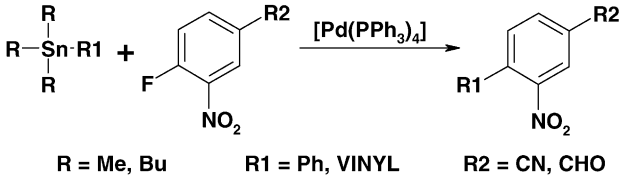

Fig. 41. Stille coupling reactions using $[Pd(PPh_3)_4]$ [71].

$[Pd_2(dba)_3]$/2-dicyclohexylphosphino-2′-(*N*,*N*-dimethylamino)-biphenyl or $[Pd(PPh_3)_4]$ which stood out as the most effective catalyst for the amination reaction (see Fig. 40).

When the highly reactive trimethylphenyltin and 2-fluoronitrobenzene were heated at 65 °C in DMF in the presence of 10% $[Pd(PPh_3)_4]$, no Stille coupling product was detected. However, when both the *ortho*- and the *para*-positions of the fluorobenzene were occupied by electron-withdrawing groups, CN or CHO, the Stille coupling proceeded smoothly even with the less reactive tributyltin compounds.

When the activated aryl fluorides (R = CN, CHO) were heated with tributylphenyltin or tributylvinyltin at 65 °C in the presence of the expected Stille coupling products formed in moderate yields. In the absence of palladium, PPh_3 alone did not catalyze the reaction, and no coupling product was detected (see Fig. 41).

The third reaction investigated was the Suzuki coupling. When the highly activated 4-methoxyphenylboronic acid and 2-fluoronitrobenzene were subjected to the conditions of the amination reaction ($[Pd(PPh_3)_4]$, Cs_2CO_3, DMF, 65 °C), the expected Suzuki coupling product was no more than 20%. However, reacting aryl fluorides that bear strong electron-withdrawing groups at both the *ortho*- and the *para*-positions phenyl boronic acid and 4-methoxy-phenylboronic acid, afforded the Suzuki coupling product, in 33–86% yield (see Fig. 42).

In summary, when activated by strong electron-withdrawing group(s), aryl fluorides are capable of undergoing Pd(0)-catalyzed amination, Stille coupling and Suzuki coupling reactions.

The mechanism of these reactions is not known with certainty; notwithstanding, the experimental data appeared to converge on the oxidative addition/reductive elimination pathway. Oxidative addition does not have to proceed via a concerted mechanism. In the cases of electron-deficient aryl fluorides, the Pd(0) species may act as a nucleophile and displace the fluoride in an S_NAr manner to form the carbon–palladium bond. The fact that a second electron-withdrawing group is only required for Stille and Suzuki reactions (but not amination) implied that oxidative addition is perhaps not even rate determining for these processes (electron-withdrawing groups do accelerate reductive elimination).

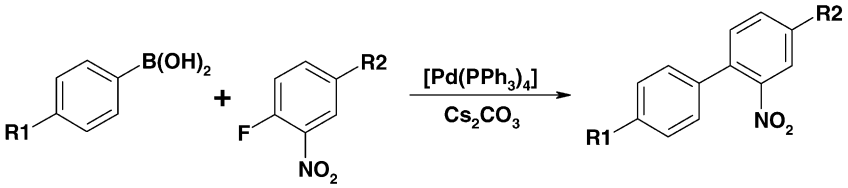

Fig. 42. Suzuki coupling reactions using $[Pd(PPh_3)_4]$ [71].

7. Platinum

Recently, Perutz and co-workers [72] published an elegant theoretical study focused on the reaction of C_6F_6 or C_6H_6 and the metal fragment [M(0)($H_2PCH_2CH_2PH_2$)] (M = Ni or Pt).

Thus, using DFT, they have explored the reaction pathways for aromatic C–H and C–F activation at 14-electron, zerovalent nickel and platinum centers. Their calculations indicate that, for both [Ni($H_2PCH_2CH_2PH_2$)] and [Pt($H_2PCH_2CH_2PH_2$)], the initial step in the reaction is the exothermic formation of an η^2-coordinated arene complex. In all cases, the complex formed with C_6F_6 is more stable than its C_6H_6 counterpart. The potential energy surface connecting the η^2-arene to the oxidative addition product is a complex one involving two distinct transition states. The metal center first migrates along the C=C bond leading to a transition state (TSb) which connects two equivalent η^2-arene structures. From TSb, the reaction coordinate follows an orthogonal mode, in which the metal center migrates along the C–X bond, leading to a transition state (TSa) where this bond is partially cleaved. The absence of a stable η^2-C–X σ complex on the potential energy surface is associated with the 14-electron configuration of the metal fragment, and distinguishes the reaction pathway from similar process involving 16-electron fragments such as [$CpRe(CO)_2$].

For both nickel and platinum, oxidative addition of the C–F bond is strongly exothermic relative to the η^2-arene complex. The kinetic barrier to bond activation is, however, significantly higher for platinum as a result of strong 5dπ–pπ repulsions in the transition state. In marked contrast, C–H bond activation is exothermic only for the platinum system. The accumulated evidence suggests that the switch from nickel to platinum has different effects on M–F and M–H bonds. Whereas the Pt–H bond benefits from improved overlap compared to nickel, the Pt–F bond is weakened by dπ–pπ repulsions. While other studies have debated the importance of attractive π bonding in metal–fluorine interactions, these studies highlight the role of repulsive π interactions.

In summary, based on these calculations, Perutz et al. predict that the nickel complex will show a strong selectivity for C–F over C–H bond activation. For platinum, in contrast, oxidative addition of both aromatic C–H and C–F bonds should be feasible, and C–H and C–F activation should be the kinetic and thermodynamic products, respectively (see Fig. 43).

Crespo et al. [73] have been interested in studies of cyclometallation reactions of platinum(II) complexes by imines. In some of these cases, reaction occurs via an oxidative addition of the C–F bond to the platinum(II) center producing a platinum(IV) complex.

The kinetics of C–X (X = H, F, Cl or Br) bond activation of ring-substituted, Arf$CH{=}NCH_2Ph$, type imines via intramolecular oxidative addition to platinum(II) complexes has been studied in acetone and toluene solution at different temperatures and pressures. Although the activation parameters determined are within the range expected, the latter is extremely large ($\Delta H^{\ddagger}$ from 25 to 70 kJ mol^{-1}, $\Delta S^{\ddagger}$ from −220 to −45 kJ mol^{-1}, $\Delta V^{\ddagger}$ from −31.2 to −9.5 cm^3 mol^{-1}). No differences were found for the reactions carried out in acetone or toluene, indicating that no polar transition state is formed during the reaction and that a common highly ordered three centered C–Pt–X interaction is present for all the imines used. A good correlation was also obtained for the $\Delta S^{\ddagger}$ and $\Delta V^{\ddagger}$ values, independent of the solvent used, confirming the non-polarity of the transition state. A deviation from this pattern is observed only for fluorinated imines both in acetone and toluene solutions; this result is interpreted by considering an earlier transition state for the oxidative addition of C–F that has not yet produced an important volume contraction of the platinum center despite the important spatial organization of the ligand, as shown by the very negative values of $\Delta S^{\ddagger}$.

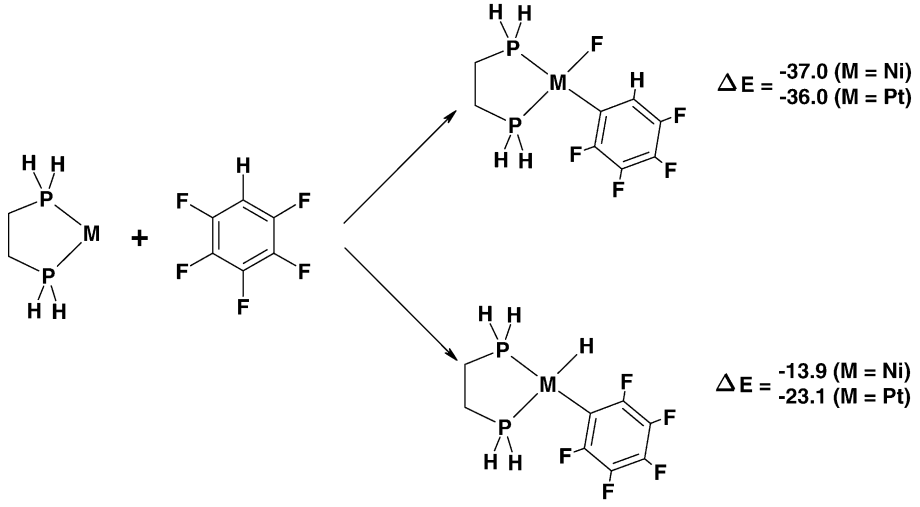

Fig. 43. Comparison of energetics of C–F and C–H activation in isomeric products (energies in kcal mol^{-1}) [72].

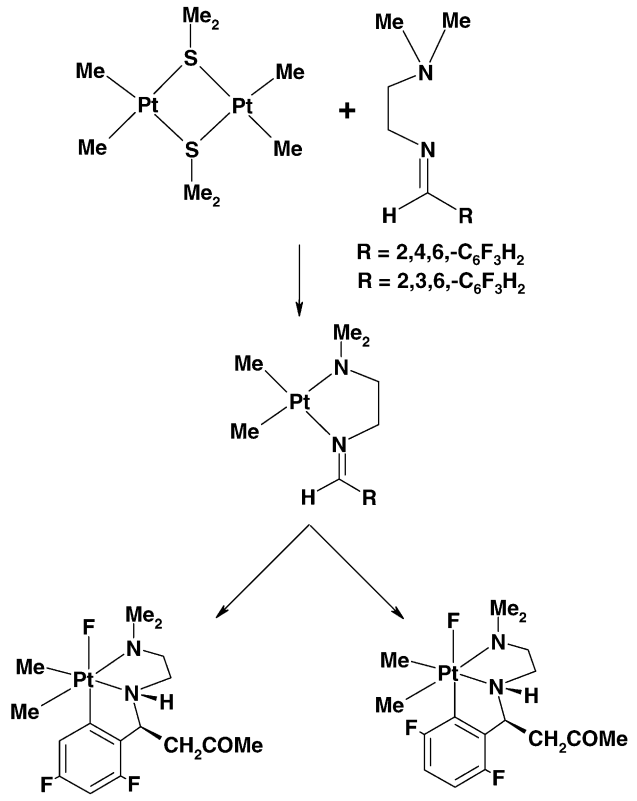

Fig. 44. Reactions of $Me_2NCH_2CH_2N{=}CHR$ (R = 2,4,6-$C_6H_2F_3$, 2,3,6-$C_6H_2F_3$) with $[Pt_2Me_4(\mu\text{-}SMe_2)_2]$ [74].

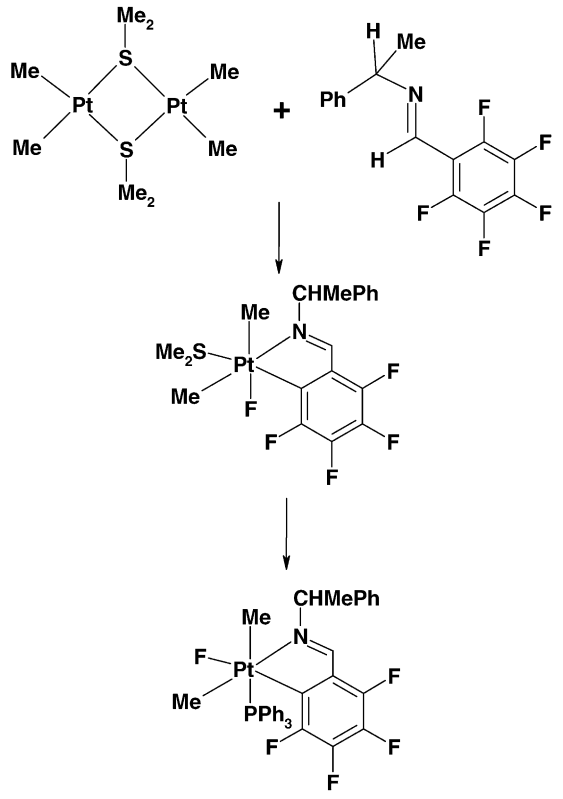

Fig. 45. Reactions of $[Pt_2Me_4(\mu\text{-}SMe_2)_2]$ with $C_6F_5CH{=}N$-(*S*)-CHMePh [75].

Crespo and co-workers [74] found that trifluorinated ligands $Me_2NCH_2CH_2N{=}CHR$ (R = 2,4,6-$C_6H_2F_3$, 2,3,6-$C_6H_2F_3$) react with $[Pt_2Me_4(\mu\text{-}SMe_2)_2]$ to yield the [C,N,N′] saturated cyclometallated platinum(IV) compounds $[PtFMe_2(Me_2NCH_2CH_2N{-}HCH(CH_2COMe)(n,m\text{-}C_6H_2F_2))]$ arising from C–F bond activation followed by acetone addition on the iminic bond of the coordinated ligand as shown in Fig. 44. $[PtFMe_2(Me_2NCH_2CH_2NHCH(CH_2COMe)(2,4\text{-}C_6H_2F_2))]$ has been characterized crystallographically.

As shown in Fig. 45 [75], the reactions of $[Pt_2Me_4(\mu\text{-}SMe_2)_2]$ with ligands ArCH=N-(*S*)-CHMePh (Ar = 2-BrC_6H_4, 2,6-$Cl_2C_6H_3$, C_6F_5, 2-FC_6H_4 and 2-$CF_3C_6H_4$) give either cyclometallated compounds $[PtMe_2X(ArCH{=}N\text{-}(S)\text{-}CHMePh)(SMe_2)]$ by intramolecular activation of C–X (X = Br, Cl or F) bonds, or compounds $[PtMe(ArCH{=}N\text{-}(S)\text{-}CHMePh)(SMe)_2]$ by *ortho*-metallation, followed by methane elimination. The reactions of these compounds with PPh_3 result in the formation of $[PtMe_2X(ArCH{=}N\text{-}(S)\text{-}CHMePh)(PPh_3)]$ or $[PtMe(ArCH{=}N\text{-}(S)\text{-}CHMePh)(PPh_3)]$, respectively. Oxidative addition of methyl iodide to $[PtMe(ArCH{=}N\text{-}(S)\text{-}CHMePh)(PPh_3)]$ produces the corresponding complexes $[PtMe_2I(ArCH{=}N\text{-}(S)\text{-}CHMePh)(PPh_3)]$. The NMR spectra of compounds $[PtMe_2X(ArCH{=}N\text{-}(S)\text{-}CHMePh)(SMe_2)]$ and $[PtMe_2X(ArCH{=}N\text{-}(S)\text{-}CHMePh)(PPh_3)]$ indicate that these are formed as pairs of diastereomers. The X-ray structure of $[PtMe(2\text{-}FC_6H_6CH{=}N\text{-}(S)\text{-}CHMePh)(PPh_3)]$ is reported [75].

Jasim and Perutz [76] found that *trans*-$[Pt(PCy_3)_2H(FHF)]$ can be synthesized by a C–F activation route. Reaction of *trans*-$[Pt(PCy_3)_2H_2]$ with hexafluorobenzene in the presence of $[NMe_4]F$ yields the bifluoride complex *trans*-$[Pt(PCy_3)_2H(FHF)]$ and *trans*-$[Pt(PCy_3)_2H(C_6F_5)]$ in a ratio of 1:13. The latter was characterized by Stone and co-workers following C–H activation of C_6F_5H with $Pt(PCy_3)_2$ [77]. A control experiment showed no reaction between *trans*-$[Pt(PCy_3)_2H_2]$ and $[NMe_4]F$.

Treatment [78] of *trans*-$[PtCl_2(PPh_{2-n}(C_6F_5)_{n+1})_2]$ ($n = 0$ or 1) with $Pb(SC_6HF_4\text{-}4)_2$ yields a mixture of monometallic *cis*/*trans* $[Pt(SC_6HF_4\text{-}4)_2(PPh_{2-n}(C_6F_5)_{n+1})_2]$, thiolate-bridged bimetallic *cis*/*trans* $[Pt_2(\mu\text{-}SC_6HF_4\text{-}4)_2(SC_6HF_4\text{-}4)_2(PPh_{2-n}(C_6F_5)_{n+1})_2]$ and $[Pt(SC_6HF_4\text{-}4)_2(1,2\text{-}C_6F_4(SC_6HF_4\text{-}4)(PPh_{2-n}(C_6F_5)_n)]$ as shown in Fig. 46.

To rationalize the outcome from these reactions, activation and cleavage of an *ortho*-carbon–fluorine bond at a phosphine ligand, transfer of a thiolate moiety and rearrangement of the parent bimetallic complexes have to be considered. Therefore the *ortho*-carbon atoms of complexes $[Pt(SC_6HF_4\text{-}4)_2(1,2\text{-}C_6F_4(SC_6HF_4\text{-}4)(PPh_{2-n}(C_6F_5)_n)]$ can be envisaged as the center of a nucleophilic attack by a thiolate–sulfur atom.

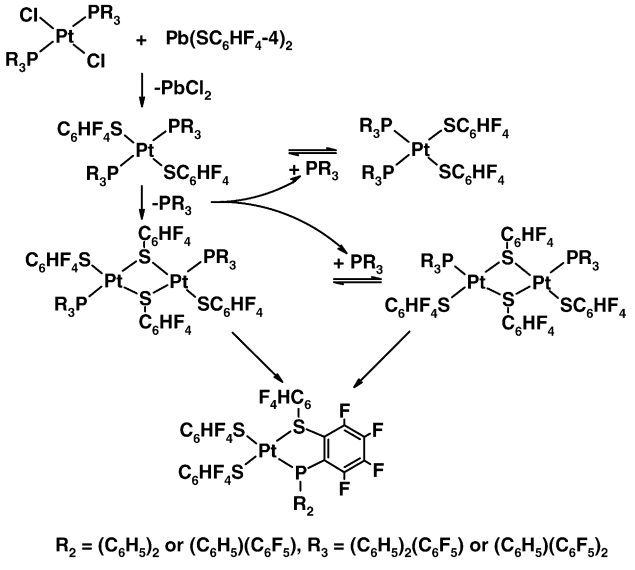

Fig. 46. Reactions of *trans*-[$PtCl_2(PPh_{2-n}(C_6F_5)_{n+1})_2$] ($n = 0$ or 1) with $Pb(SC_6HF_4\text{-}4)_2$ [78].

8. Final remarks

During the last decade, significant progress has been made in the area of metal-assisted C–F bond activation. Although a wide variety of metals are capable of activating the carbon–fluorine bond under the appropriate conditions, each family of metals has its own virtues and limitations. Thus, the fluoride affinity of the highly electrophilic early transition metals tends to afford quite robust reaction products precluding their use in catalysis, for example. Similarly, the alkali and alkaline earth metals are not suitable as C–F activation catalysts due to their propensity to form ionic salts with fluoride, even though very efficient defluorination systems are known.

Naturally, low-valent electron-rich transition metals have attracted considerable attention and several research groups have achieved surprising results in terms of chemical selectivity, mechanistic understanding and theoretical foundations.

Early efforts typically employed forcing conditions and obtained low yields. Carbon–fluorine activation can now be accomplished under extremely mild conditions using a suitable transition-metal complex.

Despite the many diverse catalytic and stoichiometric processes known today, very few of these systems are well understood. Unfortunately, many of these metal-promoted C–F activation reactions are recognized only because they form compounds in which a C–F bond has been ruptured, and typically a polyfluorinated ligand is coordinated to the metal center in the product.

Further developments in this field require a mechanistic understanding of the chemical interactions between the metal complex and the organic substrate.

As demonstrated in the preceding sections, several platinum group metal (PGM) complexes are capable of C–F oxidative addition which is one of the fundamental mechanistic steps necessary for metal-catalyzed functionalization of polyfluorinated molecules.

A large number of C–F activation reactions have been studied using fluoroolefins. Upon coordination, the fluoroolefin moiety becomes rather electrophilic as evidenced by the facile addition of protic acids. Due to this enhanced electrophilicity, coordinated fluoroolefins also tend to react readily with Lewis acids to afford vinyl complexes via fluoride abstraction. Ru [22,23], Os [30], Rh [40,50] and Ir [52,62,63] fluoroolefin complexes have been prepared and examined along with several compounds having the M–CF_2R skeleton, M = Rh, R = CF_2CF_3, C_6F_5 [44]; M = Rh, R = C_6F_5 [45]; M = Ir, R = CF_3 or CF_2CF_3 [54,55]; M = Ir, R = CF_2CF_3 or $CF(CF_3)_2$ [56]; M = Ir, R = CF_2CF_3 [60]; M = Ir, R = CF_2CF_3 [61]; M = Ir, R = CF_3 [64].

In general, the authors note that, as expected the reactions are strongly dependent upon the nature of the ancillary ligands. Very often these reactions proceed further through a carbene intermediate. Once considered a rarity, intramolecular α-fluorine elimination to afford difluorocarbene species is now a well-established procedure.

Hughes et al. have made extensive use of this process. They have found that $[RhCp^*(CF_2C_6F_5)(H_2O)(PMe_3)]^+$ [44] is cleanly transformed on standing overnight into $[RhCp^*(C_6F_5)(CO)(PMe_3)]^+$. To rationalize the formation of this carbonyl complex, the authors propose an intermediate with the carbene fragment (OH)Rh=$CF(C_6F_5)$. The analogous perfluoropropyl complex results from the treatment of $[RhCp^*I(CF_2CF_2CF_3)(PMe_3)]^+$ with silver triflate and $NaB(ArF)_4$ in the presence of water. Similarly [45] but without CO migration, $[RhCp^*I(CF_2C_6F_5)(CO)]$ undergoes rapid hydrolysis of the R–CF_2 moiety to afford the oxametallacycle $[Rh(1,2\text{-}C_6F_4(O)(CO))Cp^*(PMe_3)]$. This group has also found the first examples [54,55] of hydrogenolysis of the α-CF_2 groups in some iridium fluoroalkyls using dihydrogen under ambient condition $[IrCp^*(CF_2Rf)(H_2O)(PMe_3)]^+$ (Rf = CF_3 or CF_2CF_3) mediated by $[IrCp^*(=CFRf)H(PMe_3)]^+$ affords $RfCH_2F$ and $RfCH_3$ but no $RfCH_2F$. Similarly, $[IrCp^*(CF(CF_3)_2)(H_2O)(PMe_3)]^+$ yields $CF_3CH_2CF_3$ but no CF_3CHFCF_3. Carbene intermediates have also been found [60] in the reaction of $[IrCp^*(CF_2CF_3)(H_2O)(PMe_3)]^+$ and H_2S with $[IrCp^*(=CFCF_3)(HS)(PMe_3)]^+$ (intermediate) to yield $[IrCp^*(S(S)CHCF_3)(PMe_3)]^+$. Caulton and co-workers [26] have found that $[RuH(F)(CO)(P^tBu_2Me)_2]^+$ and Me_3SiCF_3 yields the complex $[RuH(F)(=CF_2)(CO)(P^tBu_2Me)_2]$ whereas [30] the vinyl C–F cleavage by $[OsCl(H)_3(P^iPr)_2]$ afforded $[OsCl(F)(=CHMe)(P^iPr)_2]$. Roper and co-workers [52] found that $[IrCl_2(CF_2CF_2H)(CH_3CN)(PPh_3)_2]$ reacts with HCl through the intermediate fluorocarbene complex $[IrCl_2(=CFCF_2H)(CH_3CN)(PPh_3)_2]^+$ to yield, upon hydrolysis $[IrCl_2(C(O)CF_2H)(CH_3CN)(PPh_3)_2]$. Thermolysis of the acyl complexes results finally in a migration process and formation of $[IrCl_2(CF_2H)(CO)(PPh_3)_2]$.

Fluorinated arenes have been also studied in a variety of C–F activation reaction. Perutz and co-workers [19,20] have found that *cis*-[Ru(H)$_2$(Me$_2$PC$_2$H$_4$PMe$_2$)$_2$] reacts with i.a. C_6F_6, C_6HF_5, $C_6H_2F_4$ or $C_6H_3F_3$, to generate the fluorophenyl hydride *trans*-[RuH(Rf)(Me$_2$PC$_2$H$_4$PMe$_2$)$_2$], (Rf = C_6F_5, C_6HF_4, $C_6H_2F_3$, $C_6H_3F_2$), complexes from C–F insertion exclusively. Similarly, they [76] have found that reaction of *trans*-[Pt(PCy$_3$)$_2$H$_2$] with hexafluorobenzene in the presence of [NMe$_4$]F yields the bifluoride complex *trans*-[Pt(PCy$_3$)$_2$H(FHF)] and *trans*-[Pt(PCy$_3$)$_2$H(C_6F_5)] [77]. Aizenberg and Milstein [33] found that [Rh(SiR$_3$)(PMe$_3$)$_3$] reacts quantitatively with C_6F_6 yielding [Rh(C_6F_5)(PMe$_3$)$_3$]. Treatment of this compound with HSiR$_3$ affords [RhH(C_6F_5)(SiR$_3$)(PMe$_3$)$_3$] which closes the catalytic cycle producing C_6HF_5 and restoring the catalytic precursor. Edelbach and Jones [21] found that the complex [Rh(η^5-C_5Me_5)(H)$_2$(PMe$_3$)] reacts with C_6F_6, C_6F_5H, $C_{12}F_{10}$ or $C_{10}F_8$ to give the C–F cleavage products [Rh(η^5-C_5Me_5)(aryl–F)H(PMe$_3$)]. The reaction has autocatalytic character and fluoride ion is shown to be responsible for the catalysis. A mechanism initiated by deprotonation of [Rh(η^5-C_5Me_5)(H)$_2$(PMe$_3$)] followed by nucleophilic attack of the resulting anion on the polyfluoroaromatic with subsequent loss of fluoride is proposed. The fluoride ion continues the cycle by deprotonating [Rh(η^5-C_5Me_5)(H)$_2$(PMe$_3$)].

Successful examples of chelated assisted activation of aromatic C–F bonds provided the foundation for further exploration of the organometallic chemistry of fluorocarbons. While early examples were limited to perfluorinated aromatic systems, the scope of this process is now wider and includes a variety of functionalized ligands. Thus, Murai and co-workers [46] have discovered the first Rh-catalyzed, chelation assisted Si–F exchange reaction between disilanes and fluoroarenes activated by ketone or oxazoline functionality *ortho* to the C–F bond. Esteruelas and co-workers [29] have demonstrated that [OsH$_6$(P^{i}Pr$_3$)$_2$] is capable of activating *ortho*-C–F bonds of fluorinated aromatic ketones yielding [OsH$_3$(C_6F_4C(O)R)(P^{i}Pr$_3$)$_2$] (R = CH_3, C_6F_5) and [OsH$_3$(C_6H_3FC(O)CH_3)(P^{i}Pr$_3$)$_2$]. Calculations suggest that, in agreement with the C–F activation of pentafluorobenzophenone, in aromatic ketones the C–F activation is much more favored than the C–H activation, from a thermodynamic point of view. So, the preferred C–H activation in 2-fluoroacethophenone and 2,3,4,5-tetrafluoroacetophenone appears to have kinetic origin, which could be, in part, related with the preferred *anti* arrangement of the F–C–C–C=O unit of the starting ketones. Crespo and co-workers [74,75] found that fluorinated ligands such as Me$_2$NCH$_2$CH$_2$N=CHRf (Rf = 2,4,6-$C_6H_2F_3$, 2,3,6-$C_6H_2F_3$) or C_6F_5CH=NCHMePh react with [Pt$_2$Me$_4$(μ-SMe$_2$)$_2$] to yield the [C,N,N′] saturated cyclometallated platinum(IV) [PtFMe$_2$(Me$_2$NCH$_2$CH$_2$N–HCH(CH$_2$COMe)(*n*,*m*-$C_6H_2F_2$))] or [PtMe$_2$F(C_6F_4CH=NCHMePh)(SMe$_2$)] compounds by intramolecular activation of C–F bonds. Perutz and coworkers [42] have shown that irradiation of [Rh(η^5-C_5H_5)(PMe$_3$)(C_2H_4)] in pentafluoroanisole generates the metallacycle [(η^5-C_5H_5)(PMe$_3$)RhCH$_2$OC_6F_4] used to generate [(η^5-C_5H_5)(PMe$_3$)Rh=CH(OC_6F_4)]PF_6.

Saunders and co-workers [35,36] discovered several interesting reaction involving C–F activation in the chelating phosphine (C_6F_5)$_2$PCH$_2$CH$_2$P(C_6F_5)$_2$ upon treatment with [{MCp*Cl(μ-Cl)}$_2$] (M = Rh or Ir). Activation of two C–H bonds of the Cp* ligand followed by formation of two C–C bonds affords the final product with net elimination of HF. In the absence of ethanol, thermolysis of [MCp*Cl(η^2-(C_6F_5)$_2$PCH$_2$CH$_2$P(C_6F_5)$_2$] does not lead to C–F activation, suggesting an open coordination site on the metal is required for this transformation. Interestingly, the less heavily fluorinated phosphine ($C_6H_3F_2$)$_2$PCH$_2$CH$_2$P($C_6H_3F_2$)$_2$ exhibits similar C–F activation and functionalization chemistry as described above for Rh but not for Ir. Perhaps this difference can be ascribed to the enhanced kinetic lability of second-row transition metals coupled with the increased thermodynamic stability of metal ligand bonds in the third row. These transformations are of interest since they also provide examples of net functionalization of C–F bonds to form C–C bonds. Other examples include the reactions [37] between [Rh(η^5-C_5Me_4H)Cl(μ-Cl)]$_2$ or [38] [Rh(η^5-C_5Me_4Et)Cl(μ-Cl)]$_2$ and (C_6F_5)$_2$PCH$_2$CH$_2$P(C_6F_5)$_2$ (dfppe), to yield the chiral cation [Rh(η^5-C_5HMe_2–2,4-[CH$_2$$C_6F_4$P($C_6F_5$)CH$_2$]2-1,3)Cl]$^+$ and what the authors have formulated as "[Rh(η^5-C_5Me_4Et)Cl((C_6F_5)$_2$PCH$_2$CH$_2$P(C_6F_5)$_2$)–2HF]BF_4".
The compounds [RhCl(η^5-C_5Me_5)((C_6F_5)$_2$PC_6H_4SMe-2)]BF_4, and the diastereoisomer of [RhCl(η^5-C_5Me_5)((C_6F_5)PhPC_6H_4SMe-2)]BF_4, in which C_5Me_5 and C_6F_5 are *cis*, undergo rapid coupling. The reaction between [Rh(μ-Cl)Cl(η^5-C_5Me_5)]$_2$ [41] and the tetrafluoropyridyl-substituted diphosphine Ph$_2$PCH$_2$CH$_2$PPh(C_5F_4N-4) yielding racemic diastereoisomers of [RhCl(η^5-C_5Me_5)(Ph$_2$PCH$_2$CH$_2$PPh(C_5F_4N-4))](BF_4), underwent rapid dehydrofluorinative C–C coupling to give the respective enantiomers of [RhCl(η^5,κP,κP–C_5Me_4CH$_2$–2-C_5F_3N–4-PPhCH$_2$CH$_2$PPh$_2$)]BF_4.

Monofluoro arenes are normally inert toward nucleophilic attack. However, Widdowson and Wilhelm [68,69] have found that (fluoroarene)-tricarbonylchromium(0) complexes undergo Suzuki and Stille cross-coupling reactions to form functionalized biaryl and styrene complexes in the presence of a palladium catalyst. They have also reported the first successful palladium-catalyzed Suzuki reaction of an uncomplexed fluoroarene. Mi Kim and Yu [71] have studied the palladium(0)-catalyzed amination, Stille coupling and Suzuki coupling reactions of electron-deficient aryl monofluorides. The mechanism of these reactions is not known with certainty. Experimental data appeared to converge on the oxidative addition/reductive elimination pathway. Oxidative addition does not have to proceed via a concerted mechanism. In the cases of electron-deficient aryl fluorides, the Pd(0) species may act as a nucleophile and displace the fluoride in an S_NAr manner to form the carbon–palladium bond. The fact that a second electron-withdrawing group is only required for Stille and Suzuki reactions (but not amination)

implied that oxidative addition is perhaps not even rate determining for these processes considering that electron-withdrawing groups do accelerate reductive elimination.

It is clear that several ligand-based systems show promise and should be further exploited as model compounds for systematic studies directed toward catalytic C–F bond-activation processes. The mild conditions of these transformations provide important implications for the development of homogeneous catalysts for fluorocarbon activation and functionalization. Future efforts ought to utilize these mild C–F bond cleavage processes directed toward the ultimate functionalization of the C–F bond.

Acknowledgements

Acknowledgement is made to CONACYT (44494-Q) and DGAPA-UNAM (IN119305).

References

[1] (a) R.E. Banks, D.W.A. Sharp, J.C. Tatlow (Eds.), Fluorine—The first hundred years (1886–1986), Elsevier, New York, 1986;
(b) Fluorine chemistry, Chem. Rev. Spec. Issue 96 (1996) 1555;
(c) J.S. Thrasher, S.H. Strauss (Eds.), Inorganic Fluorine Chemistry: Toward the 21st Century, ACS Editions, Washington, DC, 1994.
[2] (a) T. Hiyama, Organofluorine Compounds Chemistry and Applications, Springer, New York, 2000;
(b) B.E. Smart, in: R.E. Banks, B.E. Smart, J.C. Tatlow (Eds.), Organofluorine Chemistry: Principles and Commercial Applications, Plenum Press, New York, 1994, p. 57 (Chapter 3).
[3] (a) R.E. Banks, B.E. Smart, J.C. Tatlow (Eds.), Organofluorine Chemistry: Principles and Commercial Applications, Plenum Press, New York, 1994;
(b) R. Filler, Y. Kobayashi, L.N. Yagupolskii (Eds.), Organo-fluorine Compounds in Medicinal and Biomedical Applications, Elsevier, Amsterdam, 1993;
(c) I. Ojima, J.R. McCarthy, J.T. Welch (Eds.), Biomedical Frontiers of Fluorine Chemistry, ACS Editions, Washington, DC, 1996;
(d) A. Becker (Ed.), Inventory of Industrial Fluoro-Biochemicals, Eyrolles, Paris, 1996.
[4] Currently under scrutiny by EPA as source of perfluorooctanoic acid, C&Eng. News July 5 (2004) 6.
[5] (a) A.R. Ravishankara, S. Solomon, A.A. Turnipseed, R.F. Warren, Science 259 (1993) 194;
(b) Intergovernmental Panel on Climate Change, The IPCC Scientific Assessment, Cambridge University Press, Cambridge, 1900.
[6] S. Murai, Activation of Unreactive Bonds and Organic Synthesis, Springer, New York, 1999, pp. 243–269.
[7] T. Braun, R.N. Perutz, Chem. Commun. (2002) 2749.
[8] H. Plenio, Chem. Rev. 97 (1997) 3363.
[9] E.F. Murphy, R. Murugavel, H.W. Roesky, Chem. Rev. 97 (1997) 3425.
[10] N.M. Doherty, N.W. Hoffman, Chem. Rev. 91 (1991) 553.
[11] (a) T.G. Richmond, in: S. Murai (Ed.), Topics in Organometallic Chemistry, vol. 3, Springer, New York, 1999, pp. 243–269;
(b) T.G. Richmond, in: J.S. Thrasher, S.H. Strauss (Eds.), Inorganic Fluorine Chemistry: Toward the 21st Century, ACS Editions, Washington, DC, 1994 (Chapter 25).
[12] (a) G.C. Saunders, Angew. Chem. 108 (1996) 2783;
(b) G.C. Saunders, Angew. Chem. Int. Ed. 35 (1996) 2615.
[13] J.L. Kiplinger, T.G. Richmond, C.E. Osterberg, Chem. Rev. 94 (1994) 373.
[14] J. Burdeniuc, B. Jedlicka, R.H. Crabtree, Chem. Ber./Recl. 130 (1997) 145.
[15] H. Gérard, O. Eisenstein, J. Chem. Soc., Dalton Trans. (2003) 839.
[16] J. March, Advanced Organic Chemistry, 4th ed., Wiley, New York, 1992.
[17] R. Bosque, S. Fantacci, E. Clot, F. Maseras, O. Eisenstein, R.N. Perutz, K.B. Renkema, K.G. Caulton, J. Am. Chem. Soc. 120 (1998) 12634, and references therein.
[18] J.J. Carbó, O. Eisenstein, C.L. Higgit, A.H. Klahn, F. Maseras, B. Oelckers, R.N. Perutz, J. Chem. Soc., Dalton Trans. (2001) 1452.
[19] M.K. Whittlesey, R.N. Perutz, M.H. Moore, Chem. Commun. (1996) 787.
[20] M.K. Whittlesey, R.N. Perutz, B. Greener, M.H. Moore, Chem. Commun. (1997) 187.
[21] B.L. Edelbach, W.D. Jones, J. Am. Chem. Soc. 119 (1997) 7734.
[22] M.S. Kirkham, M.F. Mahon, M.K. Whittlesey, Chem. Commun. (2001) 813.
[23] D. Huang, J.C. Bollinger, W.E. Streib, K. Folting, V. Young, O. Eisenstein, K.G. Caulton, Organometallics 19 (2000) 2281.
[24] N.M. Doherty, S.C. Critchlow, J. Am. Chem. Soc. 109 (1987) 7906.
[25] N.W. Hoffman, N. Prokopuk, M.J. Robbins, C.M. Jones, N.M. Doherty, Inorg. Chem. 30 (1991) 4177.
[26] (a) D. Huang, P.R. Koren, K. Folting, E.R. Davidson, K.G. Caulton, J. Am. Chem. Soc. 122 (2000) 8916;
(b) D. Huang, K.G. Caulton, J. Am. Chem. Soc. 119 (1997) 3185.
[27] M. Arroyo, S. Bernès, J.L. Brianzo, E. Mayoral, R.L. Richards, J. Rius, H. Torrens, Inorg. Chem. Commun. 1 (1998) 273.
[28] M. Arroyo, S. Bernès, J.L. Brianzo, E. Mayoral, R.L. Richards, J. Rius, H. Torrens, J. Organomet. Chem. 599 (2000) 170.
[29] P. Barrio, R. Castarlenas, M.A. Esteruelas, A. Lledós, F. Maseras, E. Onate, J. Tomás, Organometallics 20 (2001) 442.
[30] G. Ferrando-Miguel, H. Gérard, O. Eisenstein, K.G. Caulton, Inorg. Chem. 41 (2002) 6440.
[31] M.D. Su, S.Y. Chu, J. Am. Chem. Soc. 119 (1997) 10178.
[32] R. Bosque, E. Clot, S. Fantacci, F. Maseras, O. Eisenstein, R.N. Perutz, K.B. Renkema, K.G. Caulton, J. Am. Chem. Soc. 120 (1998) 12634.
[33] M. Aizenberg, D. Milstein, Nature 265 (1994) 3599.
[34] M. Aizenberg, D. Milstein, J. Am. Chem. Soc. 117 (1995) 8674.
[35] M.L. Atherton, J. Fawcett, J.H. Holloway, E.G. Hope, A. Karaçar, D.R. Russell, G.C. Saunders, J. Chem. Soc., Chem. Commun. (1995) 191.
[36] M.L. Atherton, J. Fawcett, J.H. Holloway, E.G. Hope, A. Karaçar, D.R. Russell, G.C. Saunders, J. Chem. Soc., Dalton Trans. (1996) 3215.
[37] M.J. Atherton, J.H. Holloway, E.G. Hope, G.C. Saunders, J. Organomet. Chem. 558 (1998) 209.
[38] M.J. Atherton, J. Fawcett, J.H. Holloway, E.G. Hope, S.M. Martin, D.R. Russell, G.C. Saunders, J. Organomet. Chem. 555 (1998) 67.
[39] J. Fawcett, S. Friedrichs, J.H. Holloway, E.G. Hope, V. McKee, M. Nieuwenhuyzen, D.R. Russell, G.C. Saunders, J. Chem. Soc., Dalton Trans. (1998) 1477.
[40] R.M. Bellabarba, M. Nieuwenhuyzen, G.C. Saunders, Organometallics 21 (2002) 5726.
[41] R.M. Bellabarba, M. Nieuwenhuyzen, G.C. Saunders, Organometallics 22 (2003) 1802.
[42] M. Ballhorn, M.G. Partridge, R.N. Perutz, K.M. Whittlesey, Chem. Commun. (1996) 961.
[43] R.P. Hughes, T.L. Husebo, S.M. Maddock, J. Am. Chem. Soc. 119 (1997) 10231.
[44] R.P. Hughes, D.C. Lindner, A.L. Rheingold, L.M. Liable-Sands, J. Am. Chem. Soc. 119 (1997) 11544.
[45] R.P. Hughes, D.C. Lindner, L.M. Liable-Sands, A.L. Rheingold, Organometallics 20 (2001) 363.
[46] Y. Ishii, N. Chatani, S. Yorimitsu, S. Murai, Chem. Lett. (1998) 157.

[47] R.J. Young, V.V. Grushin, Organometallics 18 (1999) 294.
[48] M. Rausch, C. Bruhn, D. Steinborn, J. Organomet. Chem. 622 (2001) 172.
[49] T. Braun, D. Noveski, B. Neumann, H.G. Stammler, Angew. Chem. Int. Ed. 41 (2002) 2745.
[50] D. Noveski, T. Braun, M. Schulte, B. Neumann, H.G. Stammler, J. Chem Soc., Dalton Trans. (2003) 4075.
[51] T.R. Cundari, S. Vaddadi, Inorg. Chim. Acta 357 (2004) 2863.
[52] A.K. Burell, G.R. Clark, C.E.F. Richard, W.R. Roper, J. Organomet. Chem. 482 (1994) 261.
[53] S.D. Perera, B.L. Shaw, M. Thornton-Pett, Inorg. Chim. Acta 233 (1995) 103.
[54] R.P. Hughes, S. Willemsen, A. Williamson, D. Zhang, Organometallics 21 (2002) 3085.
[55] R.P. Hughes, J.M. Smith, J. Am. Chem. Soc. 121 (1999) 6084.
[56] R.P. Hughes, I. Kovacik, D.C. Lindner, J.M. Smith, S. Willemsen, D. Zhang, I.A. Guzei, A.L. Rheingold, Organometallics 20 (2001) 3190.
[57] R.P. Hughes, A. Williamson, R.D. Sommer, A.L. Rheingold, J. Am. Chem. Soc. 123 (2001) 7443.
[58] R.P. Hughes, R.B. Laritchev, A. Williamson, C.D. Incarvito, L.N. Zakharov, A.L. Rheingold, Organometallics 22 (2003) 2134.
[59] T.H. Peterson, J.T. Golden, R.G. Bergman, Organometallics 18 (1999) 2005.
[60] R.P. Hughes, J.M. Smith, C.D. Incarvito, K.C. Lam, B. Rhatigan, A.L. Rheingold, Organometallics 21 (2001) 2136.
[61] R.P. Hughes, D. Zhang, L.N. Zakharov, A.L. Rheingold, Organometallics 21 (2002) 4902.
[62] R.P. Hughes, R.B. Laritchev, L.N. Zakharov, A.L. Rheingold, J. Am. Chem. Soc. 126 (2004) 2308.
[63] D. Ristic-Petrovic, M. Wang, R. McDonald, M. Cowie, Organometallics 21 (2002) 5172.
[64] P.J. Albietz, J.F. Houlis, R. Eisenberg, Inorg. Chem. 41 (2002) 2001.
[65] E.D. Smurnyi, I.P. Gloriozov, Y.A. Ustynyuk, Russ. J. Phys. Chem. 77 (2003) 1699.
[66] J. Terao, A. Ikumi, H. Kuniyasu, N. Kambe, J. Am. Chem. Soc. 125 (2003) 5646.
[67] M. Jakt, L. Johannissen, H.S. Rzepa, D.A. Widdowson, R. Wilhelm, J. Chem. Soc., Perkin Trans. 2 (2002) 576.
[68] D.A. Widdowson, R. Wilhelm, Chem. Commun. (1999) 2211.
[69] R. Wilhelm, D.A. Widdowson, J. Chem. Soc., Perkin Trans. 1 (2000) 3808.
[70] D.A. Widdowson, R. Wilhelm, Chem Commun. (2003) 578.
[71] Y. Mi Kim, S. Yu, J. Am. Chem. Soc. 125 (2003) 1696.
[72] M. Reinhold, J.E. McGrady, R.N. Perutz, J. Am. Chem. Soc. 126 (2004) 5268.
[73] M. Crespo, M. Martinez, E. de Pablo, J. Chem. Soc., Dalton Trans. (1997) 1231.
[74] O. López, M. Crespo, M. Font-Bardía, X. Solans, Organometallics 16 (1997) 1233.
[75] M. Crespo, X. Solans, M. Font-Bardía, Polyhedron 17 (1998) 3927.
[76] N.A. Jasim, R.N. Perutz, J. Am. Chem. Soc. 122 (2000) 8685.
[77] J. Fornies, M. Green, J.L. Spencer, F.G.A. Stone, J. Chem. Soc., Dalton Trans. (1977) 1006.
[78] M. Arroyo, L. Villanueva, S. Bernès, H. Torrens, Chem. Commun. (2004) 1942.